Cell Reports
Physical Science

CellPress
OPEN ACCESS

Review

Heterogeneously engineered porous media for directional and asymmetric liquid transport

Guanghan Huang,[1] Xin Wei,[1] Yuheng Gu,[1] Zhanxiao Kang,[1] Lihong Lao,[2] Li Li,[1] Jintu Fan,[1] and Dahua Shou[1,3,4,5,*]

SUMMARY

Passive regulation of liquid transport in porous media in a directional or asymmetric manner has become increasingly critical to emerging applications, such as personal moisture management, water harvesting, and liquid separation. Over the past decade, heterogeneously engineering porous materials and structures for tunable liquid transport has triggered technological revolutions in those areas based on nature-inspired design, metamaterial development, and model-driven optimization. Herein, we discuss the latest developments in directional and asymmetric liquid movement created by material and structural heterogeneity, with a focus on mechanistic models, physical mechanisms, and engineering strategies to provide an improved understanding of the controllability of the directed liquid motion. We also explore the diverse applications of enhanced fluid directionality and asymmetry, from overviewing fabrication methods to analyzing significant affecting factors, including surface wettability, pore size, and flow path profile. Current challenges and research gaps are summarized to provide a road map for potential research opportunities.

INTRODUCTION

Directional and asymmetric liquid transport (DALT) is a unique natural phenomenon, which has stimulated broad applications including personal moisture management,[1,2] water harvesting,[3,4] oil recovery,[5–11] and microfluidics.[12] Numerous natural materials and structures, such as cactus spine,[13] Nepenthes alata,[14] spider silk,[15,16] shorebird beak,[17] butterfly wing,[18] and desert scorpion setae,[19] have provided rich sources of inspirations in controllable liquid transport, as shown in Figure 1. It has been found that DALT always exists on the heterogeneous skin or surface of the natural features, where the liquid movement is directed controllably by the varied geometrical structures (e.g., size, shape, and spatial distribution) and material properties (e.g., wettability). Based on 1D and 2D DALT strategies in nature, the artificial heterogeneously engineered materials and structures in a 3D fashion have triggered scientific and technological innovations in various disciplines.

Inspired by the natural configurations, researchers have discovered that porous media with a structural gradient or a wettability gradient in thickness direction enable "smart" DALT (i.e., liquid can transfer automatically across the thickness of the porous media preferably in one direction.)[22–26] Dong et al.[27] pointed out that artificial superwetting materials also promote the technology development in directional liquid dynamics. In the literature, DALT was also named "directional wicking,"[28] "one-way water transport,"[29] or "water or fluid diode."[30–32] Such DALT systems

[1]Institute of Textiles and Clothing, The Hong Kong Polytechnic University, Hung Hom, Kowloon, Hong Kong 999077, China

[2]Sibley School of Mechanical and Aerospace Engineering, Cornell University, Ithaca, NY 14853, USA

[3]Research Institute for Intelligent Wearable Systems, The Hong Kong Polytechnic University, Hung Hom, Kowloon, Hong Kong 999077, China

[4]Research Institute for Smart Energy, The Hong Kong Polytechnic University, Hung Hom, Kowloon, Hong Kong 999077, China

[5]Lead contact

*Correspondence: dahua.shou@polyu.edu.hk

https://doi.org/10.1016/j.xcrp.2021.100710

This is an open access article under the CC BY-NC-ND license (http://creativecommons.org/licenses/by-nc-nd/4.0/).

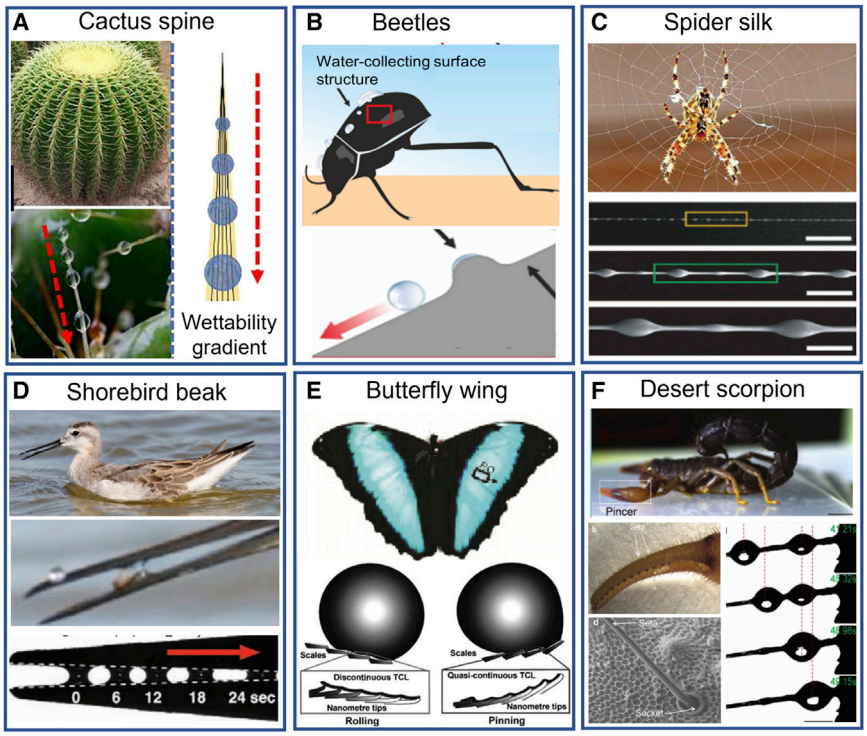

Figure 1. Representative DALT phenomena in nature

(A) Driven by wettability and structural variations, water can be transferred directionally from the tip of the cactus spine stem to the root.[13] Reproduced with permission.[13] Copyright 2020, Elsevier.

(B) A droplet is falling down directionally to the mouth of the Namib Desert Beetle[19] due to the heterogeneous wettability pattern (with hydrophilic peaks and hydrophobic valleys). Reproduced with permission.[19] Copyright 2018, American Chemical Society.

(C) On the surface of a spider silk, water droplets move from joints to spindle-knots continuously due to the Laplace pressure difference and surface energy gradient.[15,16,20] Reproduced with permission.[15] Copyright 2018, Royal Society of Chemistry.

(D) Millimetric droplets are directionally transported from the tip of a shorebird's beak to its mouth by changing the structural gradient of the beak periodically in a tweezering motion.[17] Reproduced with permission.[17] Copyright 2008, The American Association for the Advancement of Science.

(E) Due to an asymmetric structure, water droplets can easily roll off the wing of the butterfly along the radial outward direction but it is pinned in the reverse direction.[18] Reproduced with permission.[18] Copyright 2007, Royal Society of Chemistry.

(F) The fog capture process based on directional droplet movement is induced by the conical-shaped setae on the pincer of the desert scorpion.[21] Reproduced with permission.[21] Copyright 2018, John Wiley and Sons.

always have a difference of breakthrough pressures in the two opposite directions, which is determined by the thickness of the hydrophilic and hydrophobic layers, the intrinsic wettability, and pore sizes.[33]

DALT is highly crucial to many engineering processes and industrial applications, including water harvesting, personal moisture management, and liquid separation. The motivation to explore liquid water harvesting systems is to solve the water-shortage issue in arid regions. It was reported by Peng et al.[34] that fresh water accounts for only 2.5% of the total volume of water on earth and two-thirds of the global population will be suffering from water scarcity by 2025. Functional garments such as a sportswear T-Shirt with active moisture management is another emerging implementation. The directional wicking materials will irreversibly and speedily excrete sweat produced by human bodies, maintaining thermal comfort and

avoiding the breeding of bacteria.[35–37] The commercialization of scientific and research findings in moisture management–functional clothing has been increasingly growing to meet the market demands.[38] DALT-based liquid separation[39] is energy-effective and environmentally friendly, offering green and efficient solutions for distillation, wastewater treatment, and desalination.

Over the past decade, DALT in porous media has stimulated remarkable attention in various fields. Heterogeneously engineering porous materials and structures has successfully facilitated DALT based on capillary actions. It is highly desired to review and discuss the latest developments in heterogeneously engineered materials and structures for DALT. In this review, we focus on mechanisms and models to provide an improved understanding of the controllability in directed liquid motion. The technologies of DALT have been overviewed from summarizing fabrication methods and analyzing significant affecting factors to highlighting emerging applications. The current challenges and research gaps are summarized, which are helpful to provide a road map for future research opportunities. In comparison to existing reviews including superwettability-based directional liquid dynamics[40], directional flow in thin, porous materials[7], and stimuli-responsive bioinspired materials[41], the present review emphasizes the mechanisms and models of DALT in heterogeneous porous materials, based on which we present and discuss the latest fabrication methods and applications, and summarize the research challenges. The schematic view of this review's organization is presented in Figure 2. Section 2 is devoted to the fundamental and underlying mechanisms of DALT induced by gradient wettability and structure and the mathematical modeling of DALT in terms of capillary filling time and breakthrough pressure, analyzing significant affecting factors including surface wettability, geometric structure, and flow path profile. Section 3 introduces the fabrication methods of heterogeneously engineered porous materials and structures for DALT, including chemical vapor deposition, UV irradiation, photolithography, and electrospinning; and the emerging applications, such as functional clothing, water harvesting, and oil/water separation, in detail. The existing challenges are discussed and the future research opportunities are suggested in the last section.

RESULTS AND DISCUSSION

Mechanisms and models

Mechanisms and models of directional liquid transport

Understanding the mechanisms of liquid transport is significant to design, fabrication, and optimization of the DALT porous systems. The mechanisms can be mainly classified into three types as follows (i.e., wettability gradient, structural gradient, and combination of both as shown in Figure 3):

(1) Wettability gradient

In many natural phenomena,[13,19] the driving force of the DALT is induced by the wettability gradient. The wettability gradient of a solid surface can be triggered by a roughness gradient or surface-tension gradient. The liquid tends to move from the side with the lower surface energy to the side with the higher level (or better wettability), as presented in Figure 3A. The Janus wettability indicates the opposite wettability on different sides of thin, porous materials.[49] On the upward hydrophobic side, the liquid is subjected to both capillary force of the hydrophobic region (HOF) and hydrostatic pressure (HP). Here, the HOF is the capillary force induced by the convex meniscus on a hydrophobic surface, which hinders the filling of liquid into the channel.[49] The large Laplace pressure difference generated by the Janus wettability leads to the anisotropic liquid penetration. The HOF is supposed to resist the downward penetration while the HP tends to drive the liquid to move. Once the

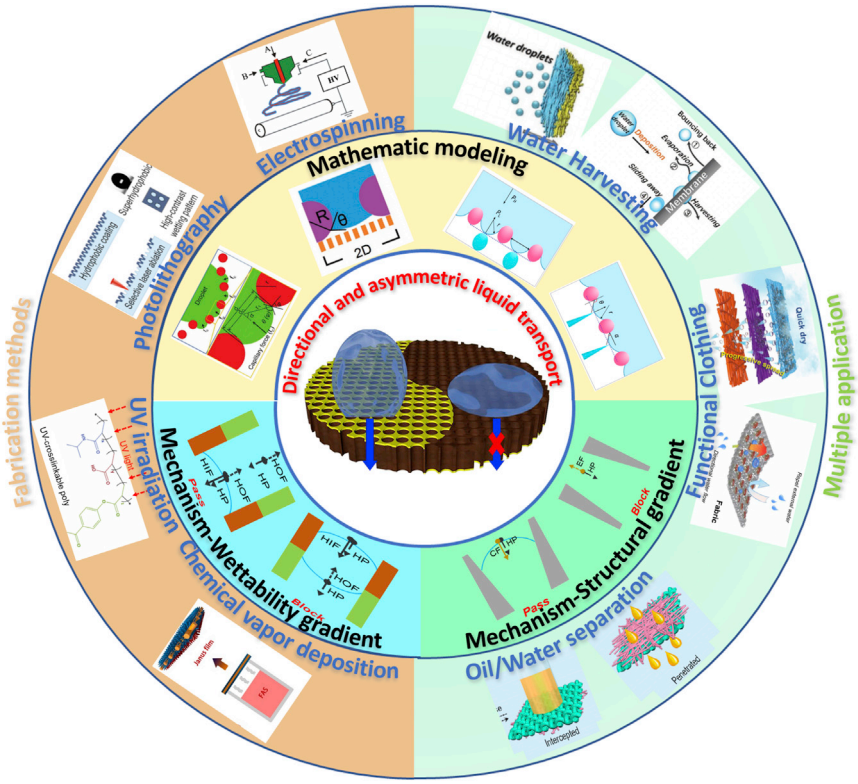

Figure 2. Schematic overview of DALT in porous media

DALT design is reproduced from Luo et al.[13] with permission. Copyright 2020, Elsevier. Mathematic model design is reproduced from Hou et al.,[42](Copyright 2019, American Chemical Society) Shi et al.,[43](Copyright 2019, John Wiley and Sons) and Choi et al.[44](Copyright 2009, John Wiley and Sons) with permission. Chemical vapor deposition design is reproduced from Shang et al.[45] with permission. Copyright 2017, John Wiley and Sons. UV irradiation design is reproduced from Shou et al.[46] with permission. Copyright 2018, John Wiley and Sons. Photolithography design is reproduced from Kostal et al.[19] with permission. Copyright 2018, American Chemical Society. Electrospinning design is reproduced from Duan G. et al.,[47] with permission. Copyright 2019, John Wiley and Sons. Water harvesting design is reproduced from Wu et al.[4] with permission. Copyright 2019, John Wiley and Sons. Functional clothing design is reproduced from Miao et al.[35] and Lao L. et al.[2] with permission. Copyright 2018, John Wiley and Sons. Copyright 2020, (retain the right of this paper as one of the authors) American Association for the Advancement of Science. Oil/water separation design is reproduced from Hou et al.[42] with permission. Copyright 2019, American Chemical Society.

liquid reaches the hydrophilic field, the capillary force provided by the menisci and the HP facilitates the liquid advance continuously. From the upward hydrophilic side, the liquid spreads with the capillary action. When the liquid reaches the Janus interface, the HOF provided by the hydrophobic interface resists further penetration of the liquid.

External stimuli such as temperature gradient can also lead to varied wettability. A double-sided synergetic Janus textile could be switched by the temperature change for the directional and regulated liquid transport, which was caused by the reversible wetting gradient and pore size change of the crosslinked lower critical solution temperature (LCST) and upper critical solution temperature (UCST) polymer networks on the two sides.[50] In addition, the fabric coated with photosensitive TiO_2 achieved self-propelled directional wicking based on the thermally-induced superhydrophobicity and the light-induced superhydrophilicity.[51]

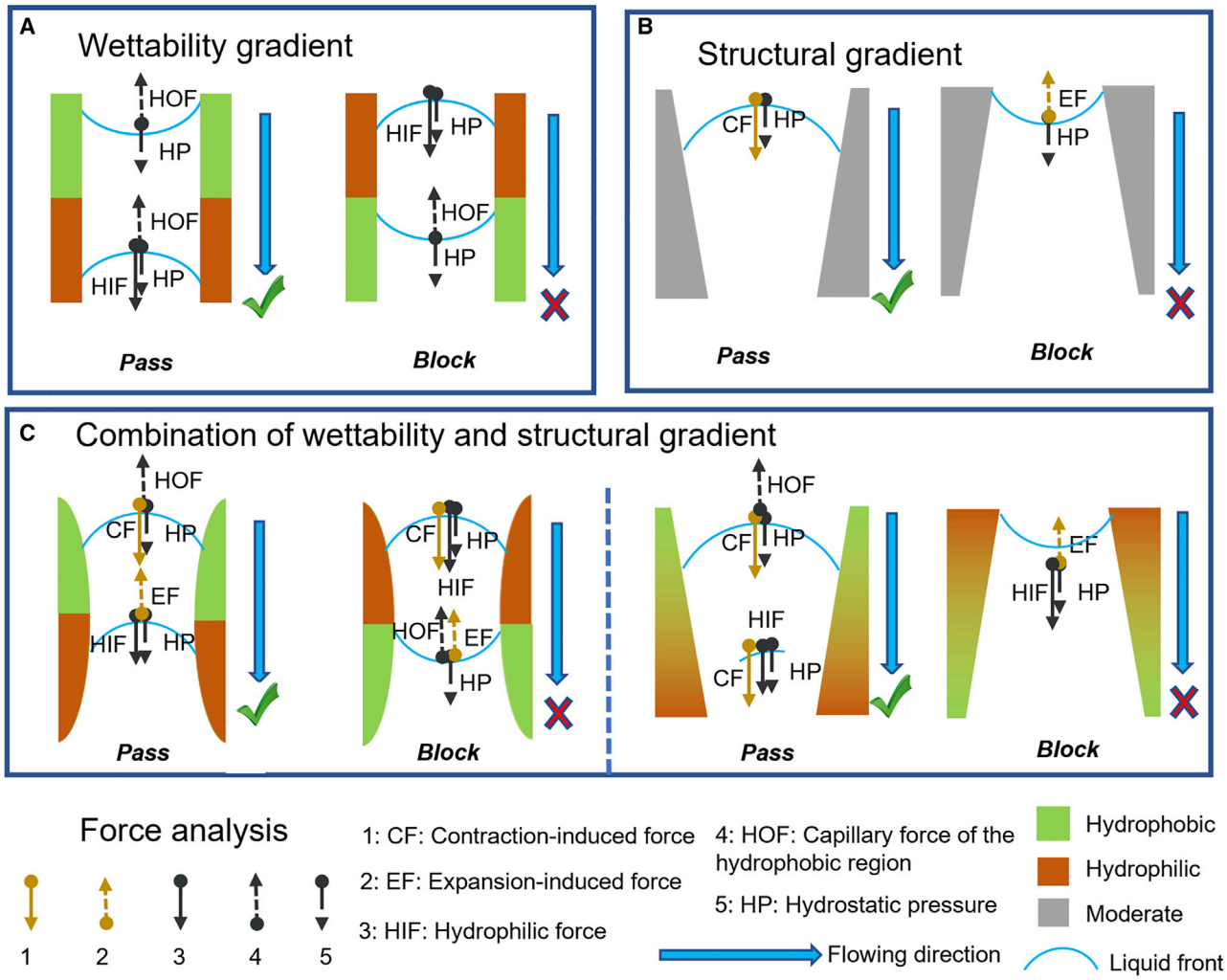

Figure 3. Mechanisms of directional liquid transport in heterogeneous porous systems with varied wettability and structure

(A) Liquid passes a hollow channel from the hydrophobic side to the hydrophilic side, but it is blocked in the opposite direction.

(B) Liquid is transported in the direction of contraction but blocked in the expansion direction.[48]

(C) Directional liquid transport is facilitated in a channel with the synergy effect of wettability and structural gradient.[2]

(2) Structural gradient

The structural gradient is another underlying cause to the flow directionality, which usually works in the artificial materials and structures.[14,52] The directional liquid transport is driven by the Laplace pressure due to the curvature and size difference,[53,54] as shown in Figure 3B. The driving pressure of a droplet inside a cone can be expressed as follows:[40]

$$\Delta P = -\left(\frac{4\gamma\cos\theta}{x_B\alpha_s} - \frac{4\gamma\cos\theta}{x_A\alpha_s}\right) \quad (1)$$

where θ is the contact angle, γ is the liquid surface tension, α_s is the semiapex angle of a cone, x is the distance between the liquid surface and the apex of the cone. In particular, x_A is the distance between the inner three-phase junction and the conical tip, x_B is the distance between the outer three-phase junction and the conical tip.

The general model of the local capillary pressure in a channel, which approximately represents a porous medium, can be derived based on thermodynamic principles.

For the channel without wedges, the capillary pressure (P_c) can be expressed as a function of relating area, perimeter, contact angle, and surface tension,[55]

$$P_c = \gamma cos\theta P_{per}/A_c, \quad (2)$$

where A_c is projected area of the terminal meniscus and P_{per} is the perimeter. The pressure difference across the liquid in a heterogeneous porous media can be calculated based on Equation (2) and used to determine the breakthrough pressure and indicate the flow direction.

(3) Combined wettability and structural gradient

Enhanced directional liquid transport can be achieved with the synergy effect of wettability and structural gradient. The corresponding mechanism has been preliminarily explored in the skin-like fabric,[2] as illustrated in Figure 3C. The Gibbs pinning criterion[56] was extended to determine the DALT status in the hollow gaps between yarns, based on the combined wettability and structural gradient on the curved wall surface. Continuous advancement of the liquid can be achieved based on the following relationship:

$$\beta = \alpha + \theta - \frac{\pi}{2} < 0 \quad (3)$$

where β is the direction angle, and α is the expansion/contraction angle of the flow path. In the positive direction ($\beta < 0$), the liquid-air interface is concave with dragging force toward the flow direction. In the negative direction ($\beta > 0$), the contact line gets pinned based on the Gibbs pinning condition.

Mechanisms and models of asymmetric liquid transport

The mechanism and models of asymmetric liquid transport are crucial to characterize the unique flow manner and the optimization design of the functional porous media. The mechanistic models in literature focus on predicting the filling time and breakthrough pressure of the porous systems with heterogeneous structures. Optimization and regulation for differential liquid absorption or transport from different flow directions are highly desirable in many applications including oil recovery, spacecraft life-support systems, moisture management fabrics, medical wound dressings, and microfluidic devices.

(1)Asymmetric transport time

Asymmetric liquid transport indicates variations in flow velocities in the opposite flow directions of the channel or porous system. The mathematical modeling of liquid absorption time has been proposed, which provides a significant theoretical basis for optimizing the size of multilayer porous media for the fastest liquid transport in one direction and the slowest one in the opposite direction. Shou et al. proposed the normalized liquid absorption time in the two-section hollow medium (Equation 4),[57] the three-section hollow medium (Equation 5), and the trapezoidal porous medium (Equation 6),[58] of which the structure configurations are presented in Figure 4, which are given by

$$R_{two-section} = \frac{1}{1-E}\left\{2\frac{mn(1+mn)(1+mn-E-nE)^2}{(1+n)^4(1+mn-mE-mnE)} + \frac{n^2(1+mn)(1+mn-mE-mnE)}{m^2(1+n)^4} + \frac{(1+mn)(1+mn-E-nE)}{(1+n)^4}\right\} \quad (4)$$

$$R_{three-section} = \frac{1}{(2+n_{32})^2} + \frac{1}{(2+n_{32})^2} + \frac{n_{32}^2}{(2+n_{32})^2} + \frac{2m_{21}}{(2+n_{32})^2} + \frac{2m_{31}n_{32}}{(2+n_{32})^2} + \frac{2m_{32}n_{32}}{(2+n_{32})^2} \quad (5)$$

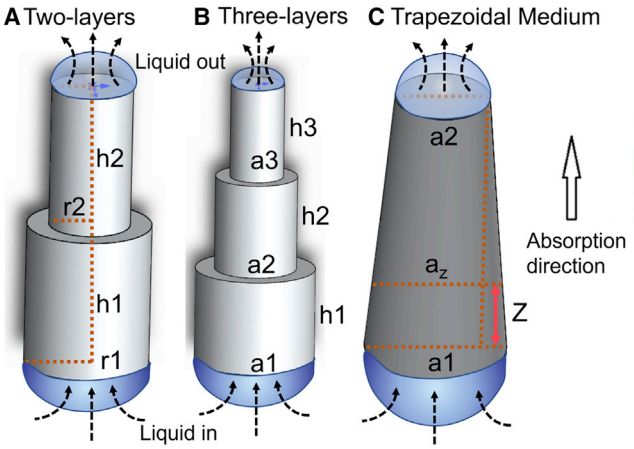

Figure 4. Schematic of heterogeneous porous systems
(A–C) Two-section medium (A), three-section medium (B), and trapezoidal medium (C) for asymmetric liquid absorption.[57,58]

$$R_{trapezoidal} = \frac{a_1^2}{2(a_1 - a_2)^2}\left\{\left(\frac{a_2^2}{a_1^2}\right)\left[ln\left(\frac{a_2^2}{a_1^2}\right)\right] + 1\right\} \quad (6)$$

respectively, where E is the porosity, n is the thickness ratio of the two layers, h is the length, r is the radius, a is the width, n_{ij} is the thickness ratio of i layer *to* j layer, and n_{ij} is the capillary radius ratio of i layer *to* j layer.

(2)Asymmetric breakthrough pressures

Breakthrough pressure is the minimal pressure required for a liquid to pass through the medium, which can be used to characterize the fluid directionality. In many cases, a high breakthrough pressure from one direction and a low breakthrough pressure (close to zero) from the other direction is highly desired. For personal moisture management, a high breakthrough pressure indicates that the face side of the fabric can resist the external liquids such as rain or contaminated water, but a low breakthrough pressure from the skin side will facilitate the sweat to wick and escape quickly. For liquid separation, a high breakthrough pressure to a certain liquid is expected to selectively filtrate or separate the blended liquids. However, a higher breakthrough pressure implies that the DALT porous media contain a greater fraction of the hydrophobic materials or a smaller pore size, which can increase the flow resistance to the liquid from the penetration direction. To sum up, the researchers are often working to find a greater difference in breakthrough pressure from the two opposite directions that indicates the greater fluid directionality. Nevertheless, whether a higher or lower breakthrough pressure is preferred depends on the application and its requirements.

The structural and wettability arrangement in a porous system determines the wicking performance and flow direction (i.e., non-wicking, unidirectional, or bidirectional).[30] Only an appropriate combination of different layers or components can induce the desired breakthrough pressure in the given flow direction. However, formulating a general framework that is versatile to predict the breakthrough pressure, as well as to guide the design and optimization of the liquid diodes and asymmetric valves, remains challenging.[59]

The mechanistic models of breakthrough pressure are different between single-layer and bilayer Janus media. The single-layer Janus medium is a homogeneous

Table 1. Breakthrough pressures of DALT porous systems

No.	Type of porous media	Liquid	Thickness (μm)	Breakthrough pressure (kPa)	Causes	Reference
1	UV irradiation coated pristine polyester fabric	Water	512	2.1-2.3	Switchable superphobicity/philicity in the Janus fabric	H. Zhou 2013[61]
2	UV irradiation coated pristine polyester fabric	Oil	512	1.1-2.2		H. Zhou 2013[61]
3	Trilayered PU/(PU-HPAN)/HPAN fibrous Media	Water	140	1.6	Superhydrophilic outer layer and hydrophobic inner layer	D. Miao 2018[35]
4	Asymmetrically carbonized wood slice coated with a PDMS superhydrophobic layer	Water	180	1.2	Superhydrophobic and superhydrophilic layers	Y.Q. Luo 2020[13]
5	All-hydrophilic fluid diode made from porous layers with asymmetric pore sizes	Water	500	0.11-0.18	Structural gradient asymmetric pores on all-hydrophilic porous materials	D. Shou 2018[48]
6	Single-layer PVDF-HFP nanofiber medium	Water	200	2	Super-amphiphobic/ superhydrophobic-oleophilic layers	H. Wang 2015[62]
7	Gradient fabric (by theoretical computation)	Water	100	0.6-4.6	Wettability gradient (lyophobic to lyphilic)	X. Tian 2012[33]
8	UV-irradiated/TiO_2-silica-coated polyester fabric	Water	500	1.8	Asymmetric wettability	H. Wang 2010[63]
9	E/W-PES-70% medium	Water	40	1.6	Wettability gradient (Superhydrophilicity-hydrophilicity)	Q. Zhang 2020[64]
10	TiO_2/PFOTES-finished cotton fabric	Water	300	0.2-0.6	Wettability gradient and structural gradient	L. Lao 2020[2]
11	Janus PVDF-HFP/PFDTMS ($M_{15/1}$)/$Cu(OH)_2$ layers	Formanide	10-21	1-3.5	Anisotropic wettability (lyophobic-lyophilic)	L. Hou 2019[42]
12	Janus PVDF-HFP/PFDTMS ($M_{15/1}$)/$Cu(OH)_2$ layers	Ethylene glycol	10-21	1.1-4.9		L. Hou 2019[42]

Abbreviations: polyurethane (PU), hydrolyzed polyacrylonitrile (HPAN), polydimethylsiloxane (PDMS), poly(vinylidene fluoride-hexafluoropropylene) (PVDF-HFP), ethanol in water (E/W), poly(ether sulfone) (PES)), 1H,1H,2H,2H-perfluorooctyltriethoxysilane (PFOTES), 1H,1H,2H,2H-perfluorodecyltrimethoxysilane (PFDTMS)

substrate with opposite wettability on its two sides. The bilayer Janus media are combined physically or chemically by two substrates with opposite wettability, and each substrate is pre-treated separately. The breakthrough pressure is highly sensitive to the thickness of the hydrophobic layer[59] and the pore-to-thickness ratio.[60] Therefore, the optimization of transverse fluid diodes requires delicate control of the thickness of the hydrophobic region or layer. For bilayer Janus media, the breakthrough pressure depends not only on the hydrophobic layer but also on the dimension of the gap between the two layers. The increased thickness of the gap results in a rising breakthrough pressure. The DALT porous medium often requires a compact contact between the bilayers for easy penetration of fluid.[59] The breakthrough pressures of various porous systems from the literature are listed in Table 1.

The breakthrough pressure (P_B)[42] of the arch-shaped liquid surface between the two cylindrical nanofiber fibers (Figure 5A) is given by:

$$P_B = -\frac{2\gamma_{lg}}{r_{liquid}} = \frac{2\gamma_{lg}\sin(\theta-\phi)}{R_f(\sin\phi - D^*)} \quad (7)$$

where θ is the contact angle, r_{liquid} represents the radius of the liquid meniscus, ϕ is the local geometrical angle, γ is the surface tension, R_f is the fiber diameter, and D^* is expressed as $(D+R_f)/R_f$, where the distance between the two adjacent fibers is $2D$.

For the multiple cylindrical fibers located in a packing pattern (Figure 5B), the breakthrough pressure (P_B) can be expressed by:[43]

$$P_B = \frac{4\gamma\sin[\theta(\phi)-\phi]}{d_0 + 2r(1-\sin\phi)} \quad (8)$$

where r is the nanofiber radius, d_o is the gap between two nanofibers, and $\theta(\phi)$ is the local liquid/solid contact angle.

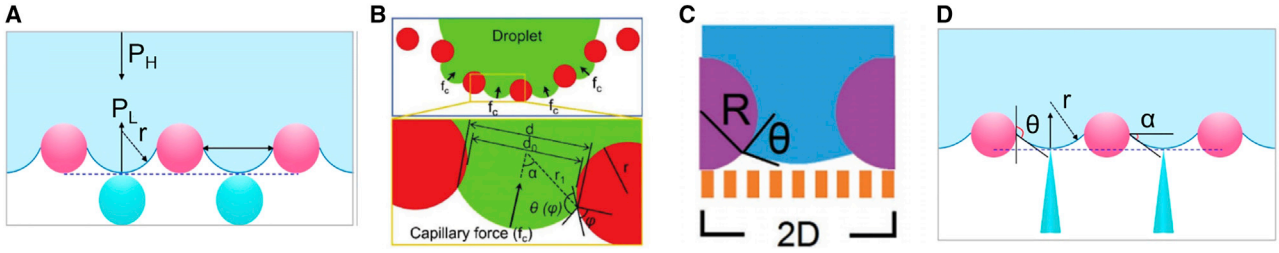

Figure 5. Laplace pressure and breakthrough pressure in various configurations of porous media

(A) Parallel cylindrical nanofiber fibers.[42] Reproduced with permission.[42] Copyright 2019, American Chemical Society.

(B) Multiple cylindrical fibers located in a packed fashion.[43]

(C) Re-entrant structure in porous layers.[44] Reproduced with permission.[43] Copyright 2019, John Wiley and Sons.

(D) Critical height of liquid water to penetrate fibers with nanoneedles.[42] Reproduced with permission.[44] Copyright 2009, John Wiley and Sons.

The breakthrough pressure (P_B) of the re-entrant structure in porous materials (Figure 5C) can be expressed as:[44]

$$P_B = \frac{2\gamma R_f}{D^2}\frac{1-cos\theta}{1+2(R_f/D)sin\theta} \quad (9)$$

where R_f is the radius of the fiber. Here, the re-entrant configuration is defined as a multivalued surface topography[44] with various local-surface curvatures.[65]

The theoretical critical height (H_c) of liquid to penetrate fibers with nanoneedles (Figure 5D) can be expressed as a function of the layer thickness:[42]

$$H_c = \frac{4\gamma_{lg}cos\theta}{n_e\rho g}\exp(\beta_f T) \quad (10)$$

where n_e indicates the nanoneedle effect, β_f is the fitting parameter, and T is the layer thickness.

A more general model of breakthrough pressure is given by:[55]

$$P_B = \frac{2\gamma}{R_{min}} + \rho g h_v \quad (11)$$

where h_v is the projected length of thickness in the vertical direction. When the breakthrough direction is upward, the value of h_v is positive. R_{min} is the minimum radius of the meniscus when the liquid is forced out in the negative direction. The R_{min} of a droplet in the cross-sections with various shapes can be derived based on the model of Mason et al. [55]

According to the above equations, the effects of material and structural parameters on the breakthrough pressure can be quantified. It has been shown that reduced fiber radii, reduced pores size, and increased thickness of the hydrophobic layer can lead to the increased breakthrough pressure. On the contrary, decreased contact angles and surface tensions of the liquid will reduce the breakthrough pressure.

Materials and fabrication of DALT porous media

Types of DALT porous media

DALT can be created mainly by wettability gradient (Figure 6A),[13] structural gradient (Figure 6B),[58,66] and switchable gradient (Figure 6C).[51] The detailed features of the three types are introduced as follows.

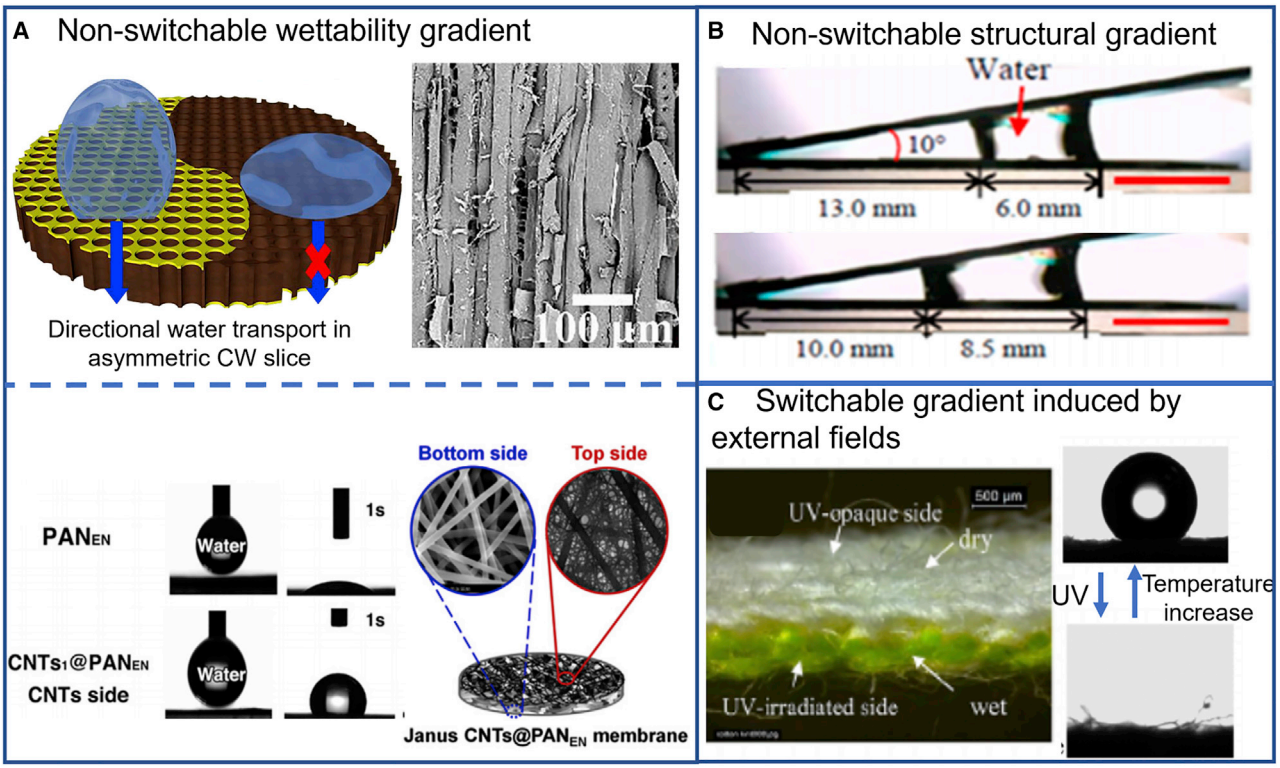

Figure 6. Typical categories of DALT porous media with non-switchable and switchable gradient

(A) Directional water transport in wood slice[13] and Janus CNTs@PAN_{EN} media with non-switchable wettability gradient.[67] Reproduced with permission.[13] Copyright 2020, Elsevier. Reproduced with permission.[67] Copyright 2017, Elsevier.

(B) Directional moving droplet toward the apex edge due to non-switchable curvature gradient.[66] Reproduced with permission.[66] Copyright 2014, American Chemical Society.

(C) Switchable wettability transition of TiO_2-coated cotton induced by the alternating temperature and UV irradiation.[51] Reproduced with permission.[51] Copyright 2018, John Wiley and Sons.

(1). Nonswitchable wettability gradient

One of the most feasible strategies to achieve DALT systems is the nonswitchable wettability gradient. Wettability gradient is typically achieved by Janus structure with a wetting contrast on the opposing sides.[45,67–72] The hydrophobic/hydrophilic Janus structure can often be fabricated in the form of a single layer,[72–75] double layers,[76] and triple layers.[35] The single-layer Janus medium can be prepared by the modification of homogeneous porous materials, such as paper, meshes, sponges, and fabrics. The bilayer Janus medium is composed of two layers with opposing wettability together and each layer can be prepared separately and then combined together.[77] The DALT porous media can also be fabricated in a tri-layer construct by introducing a transfer layer in the middle to guide the liquid transport spontaneously.[35]

(2). Nonswitchable structural gradient

The nonswitchable structural gradient often refers to the curvature gradient, including concave curvature gradient in the conical fibers,[66,73] convex curvature gradient in the tapered tubes,[78] and spiral curvature gradient in the spiral cantilevers.[79] Specifically, the asymmetric flow velocity can be achieved by the width gradient or pore-size gradient in the water channels. Shou et al.[58] studied a geometry-induced asymmetric capillary flow, where the liquid filling velocity (the depth of penetration divided by time) can be controlled by the width gradient. The fluid can

pass through the porous media faster in the direction of contraction than that in the opposite direction. The flow time for a positive gradient of cross-sectional width is much larger than that of a negative gradient at a constrained total height of the porous layers. Besides, Shou et al.[57] conducted an optimal design of contracting porous structures for rapid liquid absorption. Asymmetric flow velocity was derived in the two-layer heterogeneous porous structure and the minimum absorption time of the optimized porous structure is 38% smaller than the width-uniform control sample. Later, Shou et al.[48] proposed a novel all-hydrophilic fluid diode for asymmetric liquid flow in porous media. The fluid diode has dramatically varied pore sizes and allows capillary flow in a chosen direction from the submillimeter-size side to the submicrometer-size side.

(3). Switchable gradient

Switchable DALT can be generated on a wettability-gradient surface, which is controlled and stimulated by the external fields (Figure 6C),[51] such as temperature[50], light,[51] pH, solvent, electric field, and magnetic field.[9] Dong et al.[27] pointed out that the controllability of liquid can be significantly enhanced by applying external stimuli. The controlled wettability induced by light or temperature presented a sweating-releasing system with the TiO_2 coating on cotton fabrics.[51] The surface wettability changed from superhydrophilic to superhydrophobic and vice versa through periodic UV-exposure/heat-treatment cycles. Specifically, when the top surface was exposed to UV irradiation, the contact angle reduced from 140° to 0° while the back side remained hydrophobic.

For the wettability stimulated by electricity, Ainla et al.[80] proposed a novel electrically activated fluidic valve on the basis of electrowetting. The conductive textile is laminated by an insulator and hydrophobic layers. Without the external electric field, the liquid is unable to pass through the hydrophobic layer. With an applied voltage, the liquid penetrates the layer in one direction, which is regarded as an open valve. By incorporation of stimuli-responsive materials, smart textiles and fabrics can be developed to manipulate the liquid transport, such as controlling the flow rate, switching the on/off status, and changing the flow direction.

Substrate materials and fabrication methods

DALT porous media can be mainly divided into two types according to the material properties of the substrates (i.e., inorganic material and organic material). Inorganic materials include metal meshes or foils, graphene films, and silicon-based substrates. Organic materials generally include nonwovens, sponges, polymer membranes, natural or synthetic fabrics, and paper.

Robust Janus interfaces with DALT properties can be prepared by modifying inorganic metal materials. These sophisticated inorganic interfaces were designed by implementing biomimetic approaches. Ren et al.[73] developed an aluminum Janus system for water collection, as shown in Figure 7A. A single-layer aluminum membrane was drilled with conical micropore arrays using a femtosecond laser. Then, the membrane was treated to be superhydrophobic by utilizing a fluorosilane solution, and the backside was scanned by laser to regain hydrophilicity. Fast transport of water droplets across the aluminum membrane was realized unidirectionally. Hu et al.[77] developed a novel copper mesh hybrid Janus medium by the coupling of asymmetric topography and Janus wettability. The Janus medium is composed of a copper mesh decorated by hydrophilic nanoneedle arrays and a thin hydrophobic nanofiber layer. The nanoneedle arrays were fabricated into the micropores on the nanofiber layer, inducing a Laplace pressure difference and accelerating the DALT

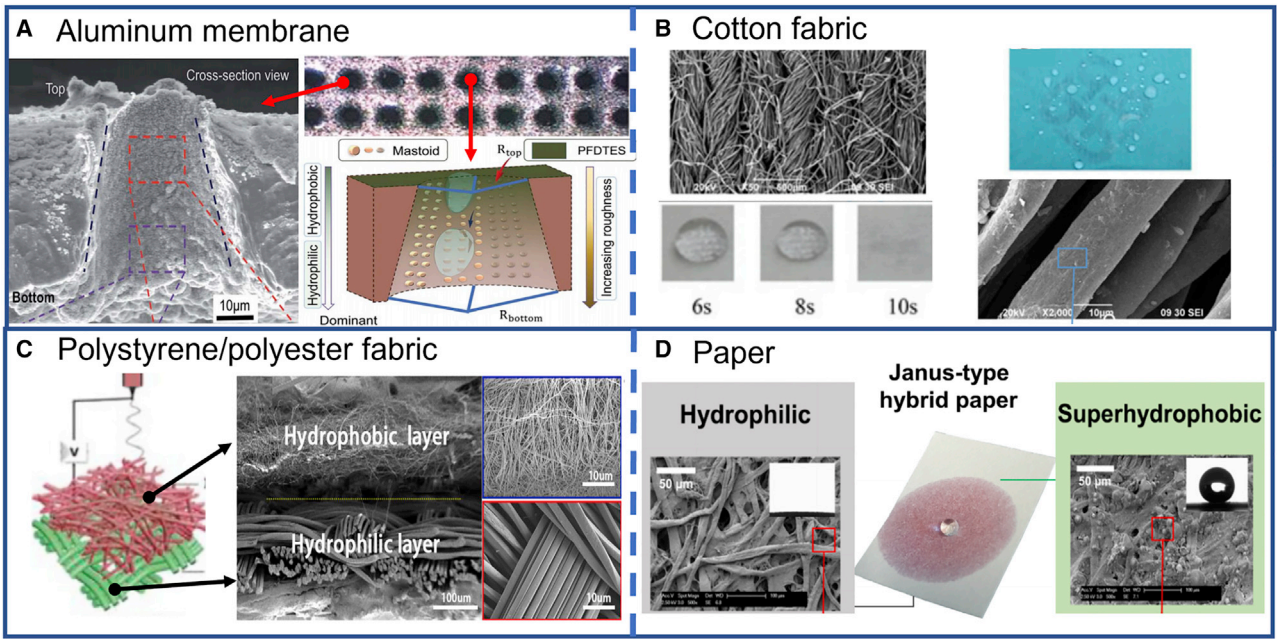

Figure 7. DALT porous media by inorganic materials and organic materials

(A) Inorganic Janus aluminum media consisting of conical pores with Laplace pressure and wettability gradient.[73] Reproduced with permission.[73] Copyright 2017, Royal Society of Chemistry.

(B) Organic Janus cotton media with TiO_2 coated on one side for unidirectional transport of water droplets.[51] Reproduced with permission.[51] Copyright 2018, John Wiley and Sons.

(C) Organic bi-layered Janus polyester fabrics with alkali treatment and deposited polystyrene solution.[76] Reproduced with permission.[76] Copyright 2019, Elsevier.

(D) Organic Janus paper sheets with superhydrophobic-hydrophilic properties.[81] Reproduced with permission.[81] Copyright 2018, American Chemical Society.

from the hydrophobic side to the hydrophilic side. As a result, effective droplet collection can be realized by the Janus system with the wettability and topography synergy.

The Janus porous media are widely developed based on organic materials such as textiles, as shown in Figures 7B–7D. Lim et al.[82] reported the organic "Janus fabric" early in 2010, though the first patent of Janus textiles in 1978 was more like a waterproof laminate without directional liquid transport properties.[38] Currently, organic Janus textiles facilitate effective implementation of directional water and sweat flow[6,51,61,83] and selective liquid absorption and separation.[38,84–88] The Janus textiles can be generally developed by commercial materials, which are detailed as below:

(1) Cotton fabric is one of the most common materials for organic Janus media,[51,84] as shown in Figure 7B. Prabu et al. developed a Janus cotton fabric by coating a hydrophobic fluoroalkyl acrylate copolymer using electrospray.[84] A water contact angle above 140° was presented on the side of the fabric with the spraying treatment, whereas the nontreated layer on the other side preserved its hydrophilicity and water wicking property. High one-way transport index values and overall moisture management grades of the cotton fabric were achieved. Later, Kong and Xin[51] proposed a multistep procedure for the DALT cotton fabric. TiO_2 particles were first coated and cured on the cotton fabric to achieve superhydrophobicity. Then, one side of the fabric surface was photoirradiated with UV light to convert

superhydrophobicity to hydrophilicity. The hydrophilic side can effectively absorb water from the hydrophobic side by the strong wicking capability, enabling the directional liquid movement.

(2) Polystyrene/polyester[76] and cellulose acetate[28] are also widely used organic substrate materials of Janus fabric media. Huang et al.[76] prepared a unique Janus fabric composed of hydrophilic polyester and hydrophobic polystyrene by electrospinning. The commercial nonwoven and woven fabrics were combined on the same layer and the thicknesses was changed to control the directional water transport capability. Besides, Babar et al.[28] reported a highly facile approach to develop DALT textiles with high water–vapor transmission and good directional moisture-transport property. Electrospun cellulose acetate mat was first subjected to the hydrolysis treatment and reactive dyeing processes, which modified the moderately hydrophobic cellulose acetate fibers into uniformly superhydrophilic fibers. Afterward, a layer of cellulose acetate mat was electrospun onto the dyed nanofiber medium.

(3) Nonwoven and paper sheets have also been utilized as DALT materials. Few studies of DALT paper sheets have been reported in literature, although the paper has an optimized industrial production process and a mature fabrication route.[89] Janus wettability paper sheets (as shown in Figure 7D) can be prepared by coating PDMS and inorganic particles, presenting high chemical durability, flexibility, and mechanical stability.[90,81]

Based on the analogous mechanistic strategy, the preparation techniques of DALT porous media include, but are not limited to, chemical or physical vapor deposition,[51,45,73,83] chemical reaction, electrospraying, photolithography,[19] plasma/laser treatment,[51,73] float coating[91], microcontact printing[92], electrospinning,[28,76,93] chemical solution deposition,[94] chemical treatment,[73,95,96] and UV irradiation,[46] as shown in Figure 8. The advantages and disadvantages of fabrication techniques are summarized and discussed in Table 2.

The DALT fabrics have presented excellent mechanical performance with a high tensile strength. Ju et al.[105] developed a double-layer, breathable and waterproof material by electrospinning techniques, which presented high tensile strength (2.9 MPa) with unidirectional moisture transport properties. Gorji et al.[106] prepared a dual-mode hydrophilic-hydrophobic polyurethane/poly(2-acryloylamido-2-methylpropanesulfonic acid)-graphene oxide (PU/P(AMPS-GO)) nanofibrous system for directional moisture transfer, showing a high tensile strength of 3.0 MPa. Liang et al.[91] proposed the polystyrene/polyethylene terephthalate/polyvinyl alcohol (PS/PET/PVA) tri-layered fabrics, which also manifested excellent mechanical strength. The tri-layered Janus media were fabricated by introducing a thin polyester fabric layer as the intermediate supporting structure for improving the mechanical strength.

Implementations and applications

Various porous media for DALT have been developed in the past decade, presenting promising applications in functional clothing (Figure 9A),[35] moisture management textile (Figure 9B), fog harvesting (Figure 9C)[52], oil/water separation (Figure 9D),[72] humidity sensor,[90] microfluidic devices,[12,54] liquid pump,[107] and condensers.[96,108] The emerging applications are highlighted and discussed as follows.

Personal moisture management

Fast-wicking textiles with profiled fibers and high wettability can drain liquid sweat away from the skin quickly by capillary action. However, such textiles are unable to

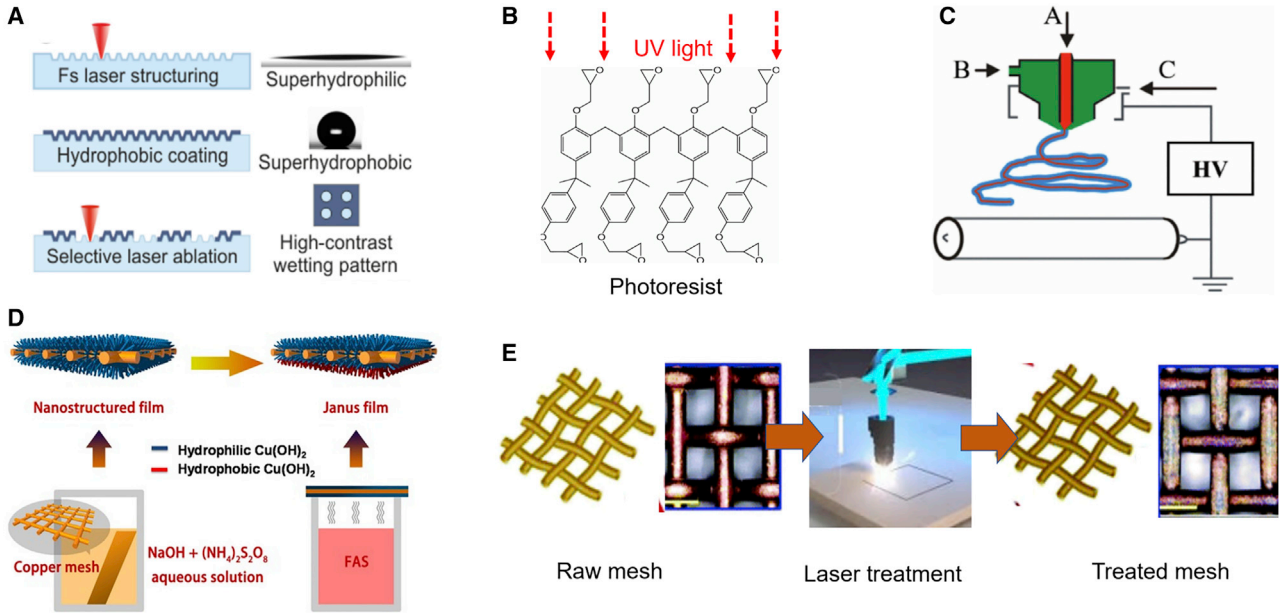

Figure 8. Fabrication techniques of DALT materials and structures

(A) Photolithography on the basis of femtosecond lasers.[19] Reproduced with permission.[19] Copyright 2018, American Chemical Society.

(B) UV irradiation for synthesis of UV-cross-linkable polymer and control of the wettability.[46] Reproduced with permission.[46] Copyright 2018, John Wiley and Sons.

(C) Coaxial electrospinning process with air-blow-assisted design.[47] Reproduced with permission.[47] Copyright 2019, John Wiley and Sons.

(D) Chemical vapor deposition on a copper mesh.[45] Reproduced with permission.[45] Copyright 2017, John Wiley and Sons.

(E) Laser treatment process on wire mesh.[5] Reproduced with permission.[5] Copyright 2017, Royal Society of Chemistry.

prevent water penetration in the reverse direction since they are homogeneous in the wettability and structure. DALT textiles with excellent wicking properties can provide a quick-drying effect in the humid and hot environment via directional transport of droplets and fluids such as sweat from the body to the environment, creating a comfortable microclimate around the body.[109]

DALT textiles used in functional clothing are generally composed of a hydrophobic outer layer and a hydrophilic inner layer. The inner layer allows water wicking but prevents diffusion of oily substances. The outer waterproof laminates have the function of "breathing,"[110] allowing the water vapor to escape freely. Fabrication of the durable outer layer is required for breathable rain tents and outdoor garments. An adhesive was applied to combine the inner and outer layers, casting a microporous hydrophilic layer directly on a thin hydrophobic layer. Based on the same approach, a functional Janus bandage has been developed,[43] which efficiently drains excessive biofluid away from wounds and prevents backflow simultaneously.

The growing demand of fast-wicking and quick-drying fabrics drives researchers to promote the advanced moisture-regulating properties.[111] The moisture management materials typically include high-wicking textiles, 3D warp-knitted spacer fabrics,[112] waterproof-breathable textiles,[113] and hydrophilic-modified hydrophobic textiles.[114] Among them, the high-wicking textiles can drive sweat away from the human skin along the profiled fibers by the increased capillary pressure. However, the existing moisture management textiles encounter many practical challenges. First, the skin side of the textiles will remain wetted and be clingy to the skin during moisture generation when the wearers are highly active. The clothes get heavier as one

Table 2. Advantages and limitations of fabrication methods of DALT porous media

Fabrication methods	Advantages	Limitations
Chemical or physical vapor deposition[51,45,73,83]	A variety of base materials (including metal meshes); high tolerance to the extreme environment; good stability in low and high temperatures.	High-temperature process; limited size due to chamber dimensions.
Chemical reaction[30,97]	High feasibility of a wide range of stimuli responses, e.g., magnetic field and pH; good durability; mass production; high homogeneity.	Difficulty in controlling the coating thickness and treating the local area.
Plasma treatment[98,99]	Improved and durable surface wettability; protection of the desirable bulk properties (modification can be restricted in the uppermost layers).	Poor absorbency; static change accumulation; requirement of vacuuming; size limitation; degradation of wettability.
Laser treatment[67,97,100]	Precise control of surface topography (micro and nano scales); good repeatability; good control of featured size and shape; feasibility of fabricating a scalable sample.	Requirement of complex experimental setups (e.g., vacuum chamber); potential harm to human body.
UV irradiation[46,61,101,102]	Contact-free ability; programmable fabrication with high accuracy by masks; versatile patterning; less limitation in sample sizes.	Long time treatment; potential harm to unprotected human eyes.
Electrospinning[72,103,104]	Production of thin fibers for high breakthrough pressure; adjustable pore size, thickness, and fiber diameter.	Limited suitable polymer materials; weak bonding between substrate and nanofibers; ease of peeling off.

sweats, especially in a hot environment or under a high physical or mental tension. Second, the wicking textiles are generally not repellent to liquid water from the external environment and cannot prevent the liquid backflow. Third, the water vapor permeability of those functional textiles is insufficient. Specifically, the moisture vapor transmission rate (~460 g/m^2.hour[115]) of commercially available fabrics is far less than the average sweating rate of a person under moderate exercise (~1000 g/m^2.hour). Moreover, once the outer layer of the fabric is saturated, the liquid flow rate will slow down quickly, and the breathability will be reduced. As such, the above challenges hinder the practical applications of functional textiles to transfer moisture from the body to the environment directionally.

New configurations and strategies have been proposed by facilitating DALT in functional textiles. Miao et al.[35] demonstrated a novel functional moisture-wicking textile composed of tri-layered fibrous media, as presented in Figure 9A. A hydrophobic polyurethane (PU) membrane was selected as the inner layer, and a hydrolyzed polyacrylonitrile (HPAN) membrane was treated with high wettability as the outer layer. The hydrolyzed PU-HPAN layer between the inner and outer layers provided a progressively varied wettability and acted as the water transfer middle layer. The water transport in the reverse direction was hindered by the transfer layer. Besides, Lao et al.[2] developed a "skin-like" fabric with one-way water transport properties and the ability to repel external liquids, as presented in Figure 9B. A hydrophilic cotton fabric was dipped with PFOTES and TiO_2 nanoparticles for superhydrophobicity. A selective plasma treatment was conducted using a patterned mask to form porous channels with a through-thickness wettability gradient. While these channels induce directional liquid flow, the superhydrophobic nature of the outer layer makes it expel the external liquids from the environment.

Zou et al.[1] developed a nature-inspired fabric with promising moisture management. It not only transfers excessive sweat to the outer layer of the fabric but also blocks and repels the external liquids such as rain and contaminated water. The proposed fabric with global hydrophobicity on the outer layer includes slit-like local areas treated with a discrete localized wettability gradient, using programmable plasma treatment and presenting high breathability, dry skin surface, reduced clinginess, and improved thermal comfort. However, only with difficulty could the slit-like water channels absorb the sweat uniformly distributed on the human skin and dissipate it effectively, considering the water repellence of the surrounding hydrophobic region and the capillary attraction of the water channels.

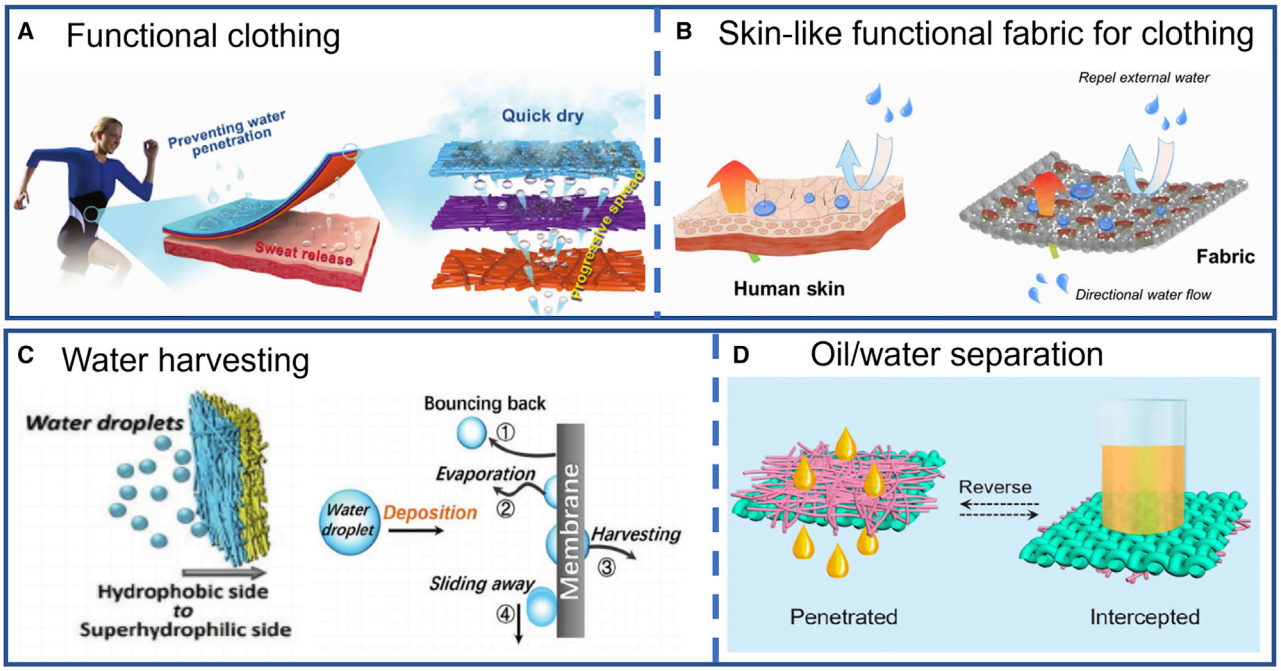

Figure 9. Emerging applications of functional porous materials with DALT properties

(A) Functional moisture management textiles for directional sweat transfer.[35] Reproduced with permission.[35] Copyright 2018, John Wiley and Sons.

(B) Skin-like functional fabric for personal moisture management.[2] Reproduced with permission.[2] Copyright 2020, (retain the right of this paper as one of the authors) American Association for the Advancement of Science.

(C) Water harvesting by a directional wicking medium.[4] Reproduced with permission.[4] Copyright 2019, John Wiley and Sons.

(D) Selective oil/water separation by inorganic or organic porous media.[42] Reproduced with permission.[42] Copyright 2019, American Chemical Society.

Water droplet harvesting

It is significant and promising to overcome the scarcity of clean water by harvesting water directly from atmospheric moisture. As shown in Figure 9C, fog harvesting based on the inspiration of nature is a significant implementation of DALT in porous systems. The Texas horned lizard and Namib Desert beetles collect dew using their structured body surface with alternating hydrophobic and hydrophilic regions.[116] These excellent water harvesting cases by natural creatures indicate the critical role of hierarchical structural gradient and wettability irregularity in DALT, and a series of hydrophobic-hydrophilic patterned fog collectors have been developed accordingly.[117] Wu et al.[4] utilized a novel hydrophobic/superhydrophilic Janus nanofibrous system to harvest water from moist air. A two-step electrospinning process was employed to fabricate directional wicking fibrous microporous media using polyacrylonitrile (PAN) as a substrate material. The Janus wicking media exhibited much greater water-harvesting efficiency than those of the same fibrous structure with the homogeneous wettability.

The working principles of water harvesting are generally based on surface wettability gradient and curvature gradient. For the wettability gradient surface, when the fog contacts the outer surface of the hydrophobic layer, small water drops will be spontaneously transported toward the hydrophilic region where they coalesce and then are collected.[61] For the curvature gradient, the presence of conical structure arrays facilitates the directional transport of captured droplets, which creates more free sites for the subsequent droplet condensation and water harvesting.[118]

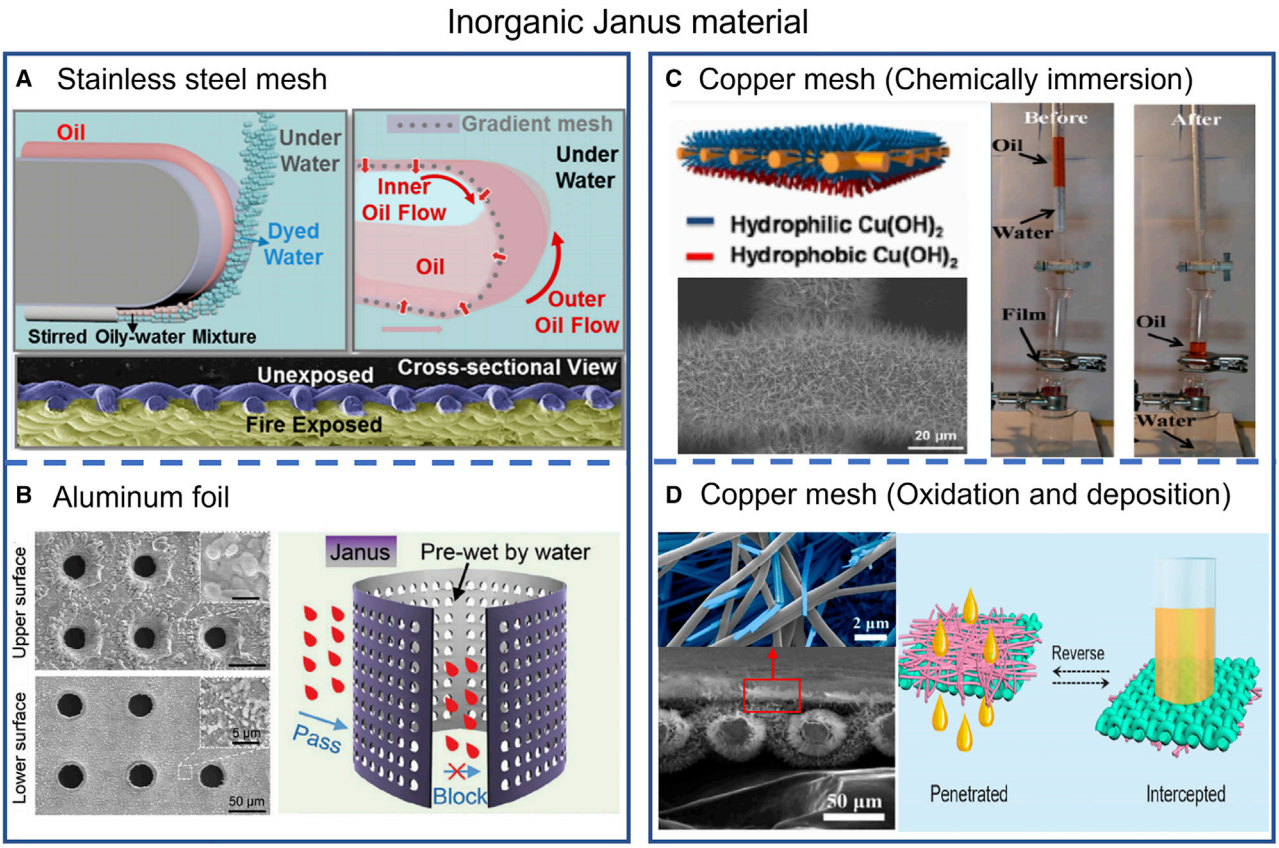

Figure 10. Inorganic DALT porous media for oil/water separation

(A) Oil/water separation by a curved stainless steel mesh with the gradient Janus wettability.[39] Reproduced with permission.[39] Copyright 2018, American Chemical Society.

(B) Janus micro-holed aluminum foil that prevents the oil from leaking outside.[68] Reproduced with permission.[68] Copyright 2017, Royal Society of Chemistry.

(C) Copper mesh substrate with $Cu(OH)_2$ nanostructure and its separation process of light oil/water mixture.[45] Reproduced with permission.[45] Copyright 2017, John Wiley and Sons.

(D) Copper mesh with $Cu(OH)_2$ nanoneedles/PVDF-HFP nanofiber that is used for directional penetration.[42] Reproduced with permission.[42] Copyright 2019, American Chemical Society.

Selective liquid separation

Liquid separation is one of the emerging applications based on DALT porous media. Vapor deposition,[39] dip coating/floating at the interface,[5,45,119–121] electrospinning,[42,71,85,122] anodic oxidation,[72] and polymer grafting[75,123] have been successfully applied to develop the DALT liquid separators. According to the substrate materials, the liquid separators can be classified into two types including inorganic and organic systems as follows.

(1). Inorganic materials for purification and separation

The oil/water separation systems have been fabricated by inorganic materials, such as copper mesh,[42,45,72] stainless steel mesh[39] (Figure 10A), glass fiber mats, and aluminum foil[68] (Figure 10B). The copper mesh is a common inorganic material for DALT membranous systems of oil/water separation. Cheng et al.[45] developed a Janus copper mesh medium for oil spill cleanup and wastewater treatment, as presented in Figure 10C. Hou et al.[42] prepared a Janus medium with a novel interpenetrating topology on copper mesh, which was reported to significantly enhance directional liquid penetration. The interpenetrating topology was readily generated

on one side of the fibrous microstructure, specifically in the valleys between the coated nanoneedles in Figure 10D. Feng et al.[72] presented an inspiring fabrication approach of Janus copper mesh for directional liquid flow, in which the copper meshes were treated with combined cathodic electrodeposition and anodic oxidation. The copper meshes can also be applied for the separation of oily liquids in a subaqueous environment.[124]

Inorganic DALT materials include stainless steel with a thin nanodendritic silica layer[39] and aluminum foil with tapered micro-hole arrays.[68] Li et al.[39] coated a gradient nanodendritic silica layer on the surface of the stainless steel mesh using chemical vapor deposition, as presented in Figure 10A. Unidirectional oil penetration through the medium was visualized by laser confocal microscopy. Zhang et al.[68] reported an efficient separation method of oil recovery, as presented in Figure 10B. The proposed system was fabricated with a Janus oil barrel and aluminum foil with tapered micro-hole arrays, where the external side was treated with the fluoroalkylsilane for superhydrophobicity. The device can efficiently extract the oil out of an oil/water mixture for oil spill remediation.

(2). Organic materials for separation and purification

DALT textiles made by organic materials offer promising solutions for oil/water separation.[6,37,75,123] The functional systems can be fabricated by various organic materials, such as cotton,[37] polyethylene terephthalate (PET) fabric,[6] polydimethylsiloxane (PDMS)/ethylene Glycol glycol (EL) fabric,[123] nanofiber,[94,122] pristine cellulose fiber,[125] paper sheet,[120] polyacrylonitrile,[67] and graphene oxide,[121] as presented in Figure 11, and the following details are provided:

(1) Polyethylene terephthalate (PET) and PET/polytetrafluoroethylene (PTFE)[30] fabrics. Zhang et al.[6] modified PET fabrics and proposed a multistep procedure to fabricate the DALT textiles for oil/water separation. In this configuration, the liquid water could rapidly penetrate the Janus media in the designed direction within seconds.

(2) Polyvinylidene difluoride (PVDF) and polyacrylonitrile (PAN)/ polystyrene (PS) nanofibers. Miao et al.[94] reported a facile approach to fabricate the DALT media with PVDF nanofiber, as presented in Figure 11A. Liang et al.[122] manufactured the DALT membranes using an electrospinning technology, with a double-layer structure including hydrophobic PS and hydrophilic PAN nanofibrous layers. The demulsification, liquid unidirectional transport, and high flux properties have been found in the electrospun DALT porous media.

(3) Pristine cellulose fibers. Yue et al.[125] coated ZnO nanorods onto the pristine cellulose fibers to enhance the surface roughness, where the efficient separation of emulsions was obtained in the DALT porous media.

(4) Paper sheet. Recently, Nau et al.[120] reported on a Janus-like hybrid system, in which eucalyptus sulfate paper sheets were coated with tetraethoxysilane (TEOS) through dipping and drying, as presented in Figure 11B. The directional penetration of oil and water from opposing directions were readily accomplished.

(5) Polyacrylonitrile. Jiang et al.[67] developed a polyacrylonitrile nanofiber system by electrospinning. A significant increase in mechanical properties, separation efficiency, and operational flux values was reported for the DALT electrospun media, on which a minor amount of CNT was deposited below several milligrams per square meter, as presented in Figure 11C.

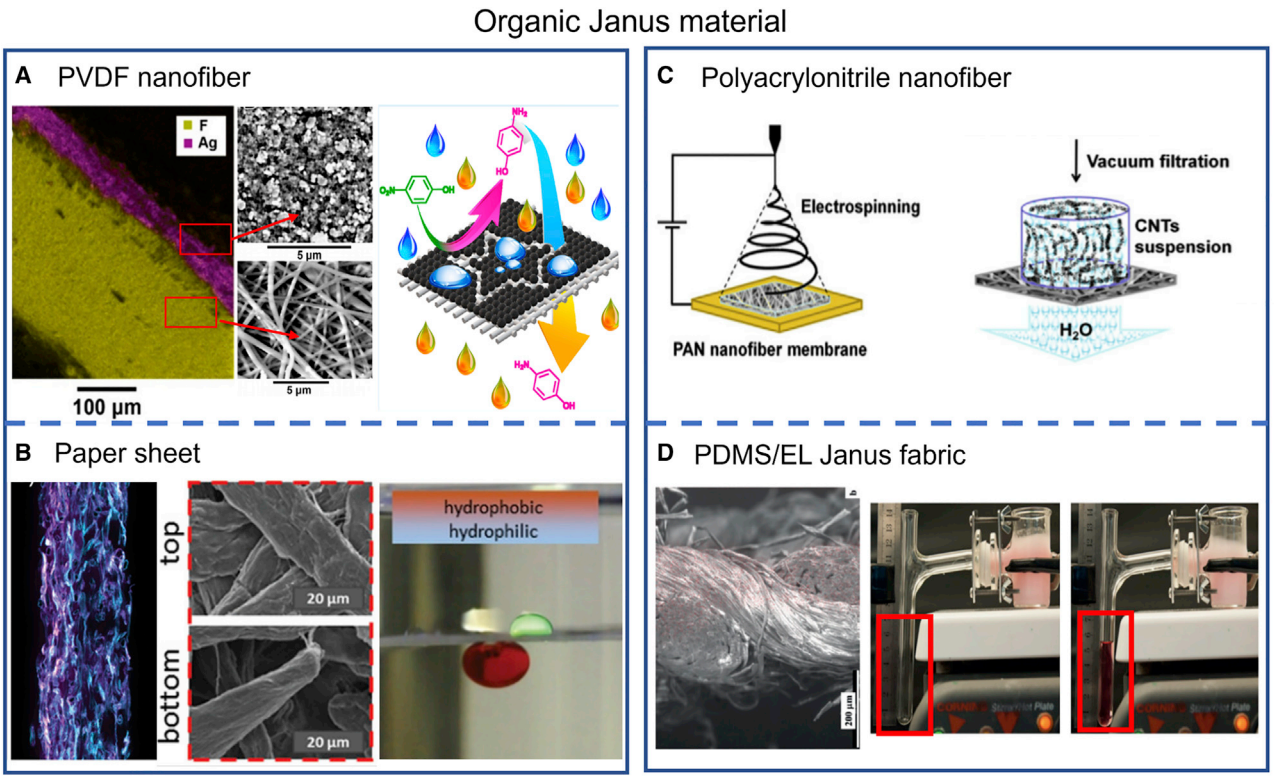

Figure 11. Organic DALT porous media for oil/water separation

(A) Separation filter by Janus PVDF media with Ag nanoparticle deposition (purple region) and Ag-free region (yellow region).[94] Reproduced with permission.[94] Copyright 2019, American Chemical Society.

(B) Silica-coated paper sheet as Janus media, where water phase lays on the hydrophilic interface.[120] Reproduced with permission.[120] Copyright 2019, John Wiley and Sons.

(C) Polyacrylonitrile nanofibrous media with high oil/water separation efficiency.[67] Reproduced with permission.[67] Copyright 2017, Elsevier.

(D) Janus fabric with polydimethysiloxane (PDMS) on one side and ethylene glycol on the other side for rapid oil separation from emulsions.[123] Reproduced with permission.[123] Copyright 2017, John Wiley and Sons.

(6) Polypropylene (PP) and polyethylene (PE). A floating solar evaporator for seawater desalination and purification[126] was developed based on a DALT nonwoven fabric composed of PP/PE core-sheath fibers. With different weight ratios of hydrophilic and hydrophobic PP/PE fibers, the Janus solar evaporator has the contact angles of 130.4° on the hydrophobic side and 35.6° on the hydrophilic side. The unique unidirectional water transfer behavior was achieved due to the wettability difference, which pumped an adjustable amount of water for the interfacial solar evaporation balanced by the water supply.

Conclusions, challenges, and perspectives

We have summarized the recent progress in the unique DALT across porous media and the underlying mechanisms. The main conclusions drawn are as follows: (1) The mechanisms of DALT can be classified as being three types including wettability gradient, structural gradient, and a combination of both. (2) The modeling and optimization of DALT focus on regulating the liquid absorbing time/velocity and breakthrough pressure, which have been comprehensively discussed to better understand the underlying mechanisms and to provide a guideline for the fabrication. (3) The main fabrication methods of the DALT porous materials and structures include vapor deposition, photolithography, chemical treatment, UV irradiation,

electro-spraying, and electrospinning. (4) The applications of DALT porous systems are concentrated on personal moisture management, water harvesting, and liquid separation.

Some fundamental challenges remain to be addressed for better implementations of DALT porous systems. Those challenges include precise capturing the liquid flow dynamics in the complex porous materials; functioning smoothly in the harsh environmental conditions; overcoming the hysteresis resistance for increased and regulated flow rates in the DALT processes; providing a facile and robust fabrication method to satisfy practical requirements, including durability, cost, and environmental friendliness; and balancing the high liquid transport capacity in the positive direction and the great breakthrough pressure in the negative direction.

First, it is difficult to capture the dynamic transport behaviors precisely in the microscale regimes inside the complex porous structures, despite the advanced visualization techniques. Accurate description of DALT phenomena and improved understanding of the underlying mechanisms are critically significant. Besides, the dynamic liquid transport phenomena in the porous systems can be affected by the various extreme environmental conditions, such as high temperature, frequent abrasion, solar aging, and high humidity—possibly leading to failure of the DALT performance.

Second, overcoming the dynamically increasing flow resistance that significantly retards the liquid transport in the DALT porous systems is another challenge. Increased and regulated flow rates are desired for different implementations such as moisture management fabrics, which are regulated to transport excessive sweat directionally and quickly. However, the hydrophobic region or the small-pore-size layer will reduce the flow velocity: the hydrophobic region will hinder the capillary flow due to the water repellence and the small pore size will reduce the fluid permeability.[127,128] As such, it is challenging but essential to increase the flow rates while maintaining the DALT behaviors. External stimuli, such as electrical, thermal, magnetic, or optical energy, are applied to accelerate the liquid flow in the smartly responsive devices.[129,130] However, in addition to the imposed external driving power, the use of various chemicals may lead to an irreversible environmental impact especially on aquatic mammals.

Third, it is extremely difficult to develop a versatile and programmable manufacturing technique to satisfy various needs.[131] Advanced fabrication techniques such as 3D printing[132,133] can be the potential candidates considering their high efficiency of translating computer-aided design into a 3D architecture in the desired manner. However, the 3D printing technology is unable to fabricate refined surfaces or structures due to the limited resolution. Moreover, 3D printing technology is limited to few materials including elastomers, thermosets, thermoplastics, and functional polymers.

Fourth, durability of the DALT porous media, including washability, abrasion durability, and chemical resistance, is critical to their long-term performance. In particular, it is highly challenging to realize robust hydrophobicity for DALT when the porous media are treated with hydrophobic-hydrophilic gradient.[134] Great efforts have been made to effectively crosslink or bond the hydrophobic coating layer onto the substrate, but the long-term durability remains a challenge.[113,135] Chemical methods have been widely applied to achieve the hydrophobicity of DALT, but the use of organic solvents may lead to safety and environmental concerns. For

example, fluorosilane or other fluorinated chemicals[73,136] are the commonly used coatings to attain durable liquid repellence. However, these chemicals including the long-chain C8 based PFOA products are under restrictions in multiple countries and regions including the United States and Europe. The fluoropolymers that remain in the environment and ecosystems have induced severe environmental issues.[137,138]

Lastly, balancing the breakthrough pressure in the negative direction and the liquid transport capacity in the positive direction is still an imperative challenge. The breakthrough pressure of the DALT porous media is often limited by the ability of liquid transport in the positive direction. Penetration of water in one direction requires larger capillary pores, which yet increases the breakthrough pressure in the other direction.[32]

By addressing the challenges, the perspectives of promoting DALT porous systems include (1) better understanding the fundamental mechanisms of DALT in the local region in the dynamic process; (2) increasing the robustness of DALT properties by structural optimization and scalable processing methods such as knitting, weaving, and high-performance 3D printing; (3) creating innovative materials that replicate nature creatures that have evolved superior configurations and features including antifouling, self-cleaning, self-healing, and stimulus-based responses; (4) extending the implementations based on the DALT porous systems, such as sweat sensing, wound dressing, and solar evaporation, and integrating the smart DALT devices with Internet of Things, Big Data, and Artificial Intelligence; (5) enhancing the DALT technologies consistently with sustainability including energy saving, carbon neutrality, green fabrication, and comfort and well-being of human beings; and (6) exploring the innovative design concepts including prewetted liquid diodes, which enable superfast liquid transport.

ACKNOWLEDGMENTS

Dr. Shou acknowledges the support from the Research Grants Council of the Hong Kong Special Administrative Region, China (Project No.: PolyU 252029/19E; PolyU 152052/21E) and the Innovation and Technology Fund of Hong Kong (Project No.: ITS/093/19).

AUTHOR CONTRIBUTIONS

All authors planned and executed the review work included in this manuscript and read/agreed to the published version of the manuscript.

DECLARATION OF INTERESTS

The authors declare no competing interests.

REFERENCES

1. Zou, C., Lao, L., Chen, Q., Fan, J., and Shou, D. (2021). Nature-inspired moisture management fabric for unidirectional liquid transport and surface repellence and resistance. Energy and Buildings. *248*, 111203.

2. Lao, L., Shou, D., Wu, Y.S., and Fan, J.T. (2020). "Skin-like" fabric for personal moisture management. Sci. Adv. *6*, eaaz0013.

3. Dai, X., Sun, N., Nielsen, S.O., Stogin, B.B., Wang, J., Yang, S., and Wong, T.-S. (2018). Hydrophilic directional slippery rough surfaces for water harvesting. Sci. Adv. *4*, eaaq0919.

4. Wu, J., Zhou, H., Wang, H., Shao, H., Yan, G., and Lin, T. (2019). Novel water harvesting fibrous membranes with directional water transport capability. Adv. Mater. Interfaces *6*, 1801529.

5. Liu, Y.-Q., Han, D.-D., Jiao, Z.-Z., Liu, Y., Jiang, H.-B., Wu, X.-H., Ding, H., Zhang, Y.-L., and Sun, H.-B. (2017). Laser-structured Janus wire mesh for efficient oil-water separation. Nanoscale *9*, 17933–17938.

6. Zhang, C., He, S., Wang, D., Xu, F., Zhang, F., and Zhang, G. (2018). Facile fabricate a bioinspired Janus membrane with heterogeneous wettability for unidirectional water transfer and controllable oil–water separation. J. Mater. Sci. *53*, 14398–14411.

7. Zhao, Y., Wang, H., Zhou, H., and Lin, T. (2017). Directional fluid transport in thin

porous materials and its functional applications. Small *13*, 1601070.

8. Hou, Y., Duan, C.-t., Zhao, N., Zhang, H., Zhao, Y.-p., Chen, L., Dai, H.-j., and Xu, J. (2016). A versatile coating approach to fabricate superwetting membranes for separation of water-in-oil emulsions. Chin. J. Polym. Sci. *34*, 1234–1239.

9. Ma, W., and Wang, H. (2019). Magnetically driven motile superhydrophobic sponges for efficient oil removal. Appl. Mater. Today *15*, 263–266.

10. Wang, F., Pi, J., Li, J.-Y., Song, F., Feng, R., Wang, X.-L., and Wang, Y.-Z. (2019). Highly-efficient separation of oil and water enabled by a silica nanoparticle coating with pH-triggered tunable surface wettability. J. Colloid Interface Sci. *557*, 65–75.

11. Luo, Y.-Q., Song, X., Song, F., Wang, X.-L., and Wang, Y.-Z. (2019). A fully bio-based composite coating with mechanical robustness and dual superlyophobicity for efficient two-way oil/water separation. J. Colloid Interface Sci. *549*, 123–132.

12. Xu, C., Feng, R., Song, F., Wu, J.-M., Luo, Y.-Q., Wang, X.-L., and Wang, Y.-Z. (2018). Continuous and controlled directional water transportation on a hydrophobic/superhydrophobic patterned surface. Chem. Eng. J. *352*, 722–729.

13. Luo, Y.-Q., Song, F., Xu, C., Wang, X.-L., and Wang, Y.-Z. (2020). Bioinspired fabrication of asymmetric wood materials for directional liquid manipulation and transport. Chem. Eng. J. *383*, 123168.

14. Chen, H., Zhang, P., Zhang, L., Liu, H., Jiang, Y., Zhang, D., Han, Z., and Jiang, L. (2016). Continuous directional water transport on the peristome surface of Nepenthes alata. Nature *532*, 85–89.

15. Li, J., and Guo, Z. (2018). Spontaneous directional transportations of water droplets on surfaces driven by gradient structures. Nanoscale *10*, 13814–13831.

16. Zheng, Y., Bai, H., Huang, Z., Tian, X., Nie, F.-Q., Zhao, Y., Zhai, J., and Jiang, L. (2010). Directional water collection on wetted spider silk. Nature *463*, 640–643. https://doi.org/10.1038/nature08729.

17. Prakash, M., Quéré, D., and Bush, J.W. (2008). Surface tension transport of prey by feeding shorebirds: the capillary ratchet. Science *320*, 931–934.

18. Zheng, Y., Gao, X., and Jiang, L. (2007). Directional adhesion of superhydrophobic butterfly wings. Soft Matter *3*, 178–182.

19. Kostal, E., Stroj, S., Kasemann, S., Matylitsky, V., and Domke, M. (2018). Fabrication of biomimetic fog-collecting superhydrophilic–superhydrophobic surface micropatterns using femtosecond lasers. Langmuir *34*, 2933–2941.

20. Feng, S., Wang, Q., Xing, Y., Hou, Y., and Zheng, Y. (2020). Continuous directional water transport on integrating tapered surfaces. Adv. Mater. Interfaces *7*, 2000081.

21. Chen, D., Niu, S., Zhang, J., Mu, Z., Chen, H., Zhang, D., Yao, Z., Han, Z., and Ren, L. (2018). Superfast liquid transfer strategy through sliding on a liquid membrane inspired from scorpion setae. Adv. Mater. Interfaces *5*, 1800802.

22. Khang, A., Ravishankar, P., Krishnaswamy, A., Anderson, P.K., Cone, S.G., Liu, Z., Qian, X., and Balachandran, K. (2017). Engineering anisotropic biphasic Janus-type polymer nanofiber scaffold networks via centrifugal jet spinning. J. Biomed. Mater. Res. B Appl. Biomater. *105*, 2455–2464..

23. Yin, K., Yang, S., Dong, X., Chu, D., Duan, J.-A., and He, J. (2018). Ultrafast achievement of a superhydrophilic/hydrophobic janus foam by femtosecond laser ablation for directional water transport and efficient fog harvesting. ACS Appl. Mater. Interfaces *10*, 31433–31440.

24. Zeng, C., Wang, H., Zhou, H., and Lin, T. (2016). Directional water transport fabrics with durable ultra-high one-way transport capacity. Adv. Mater. Interfaces *3*, 1600036.

25. Wei, X., Zhou, H., Chen, F., Wang, H., Ji, Z., and Lin, T. (2019). High-efficiency low-resistance oil-mist coalescence filtration using fibrous filters with thickness-direction asymmetric wettability. Adv. Funct. Mater. *29*, 1806302.

26. Yang, H.C., Xie, Y., Hou, J., Cheetham, A.K., Chen, V., and Darling, S.B. (2018). Janus membranes: creating asymmetry for energy efficiency. Adv. Mater. *30*, e1801495.

27. Dai, H., Dong, Z., and Jiang, L. (2020). Directional liquid dynamics of interfaces with superwettability. Sci. Adv. *6*, eabb5528.

28. Babar, A.A., Miao, D., Ali, N., Zhao, J., Wang, X., Yu, J., and Ding, B. (2018). Breathable and colorful cellulose acetate-based nanofibrous membranes for directional moisture transport. ACS Appl. Mater. Interfaces *10*, 22866–22875.

29. Wang, H., Wang, W., Wang, H., Jin, X., Li, J., and Zhu, Z. (2018). One-way water transport fabrics with hydrophobic rough surface formed in one-step electrospray. Mater. Lett. *215*, 110–113.

30. Wang, Z., Yang, X., Cheng, Z., Liu, Y., Shao, L., and Jiang, L. (2017). Simply realizing "water diode" Janus membranes for multifunctional smart applications. Mater. Horiz. *4*, 701–708.

31. Wu, M.-B., Yang, H.-C., Wang, J.-J., Wu, G.-P., and Xu, Z.-K. (2017). Janus membranes with opposing surface wettability enabling oil-to-water and water-to-oil emulsification. ACS Appl. Mater. Interfaces *9*, 5062–5066.

32. Mates, J.E., Schutzius, T.M., Qin, J., Waldroup, D.E., and Megaridis, C.M. (2014). The fluid diode: tunable unidirectional flow through porous substrates. ACS Appl. Mater. Interfaces *6*, 12837–12843.

33. Tian, X., Li, J., and Wang, X. (2012). Anisotropic liquid penetration arising from a cross-sectional wettability gradient. Soft Matter *8*, 2633–2637.

34. Peng, Y., He, Y., Yang, S., Ben, S., Cao, M., Li, K., Liu, K., and Jiang, L. (2015). Magnetically induced fog harvesting via flexible conical arrays. Adv. Funct. Mater. *25*, 5967–5971.

35. Miao, D., Huang, Z., Wang, X., Yu, J., and Ding, B. (2018). Continuous, spontaneous, and directional water transport in the trilayered fibrous membranes for functional moisture wicking textiles. Small *14*, e1801527.

36. Fashandi, H., and Ghomi, A.R. (2017). Developing breathable double-layered fibrous membranes equipped with water pulling mechanism toward clothing with enhanced comfort. Adv. Eng. Mater. *19*, 1600863.

37. Gore, P.M., and Kandasubramanian, B. (2018). Heterogeneous wettable cotton based superhydrophobic Janus biofabric engineered with PLA/functionalized-organoclay microfibers for efficient oil–water separation. J. Mater. Chem. A *6*, 7457–7479.

38. Gore, R.W., and Allen, S.B., Jr. (1980). Waterproof Laminate (Google Patents).

39. Li, N., Yu, C., Si, Y., Song, M., Dong, Z., and Jiang, L. (2018). Janus gradient meshes for continuous separation and collection of flowing oils under water. ACS Appl. Mater. Interfaces *10*, 7504–7511.

40. Cui, Y., Li, D., and Bai, H. (2017). Bioinspired smart materials for directional liquid transport. Ind. Eng. Chem. Res. *56*, 4887–4897.

41. Wang, Y., Ma, K., and Xin, J.H. (2018). Stimuli-responsive bioinspired materials for controllable liquid manipulation: Principles, fabrication, and applications. Adv. Funct. Mater. *28*, 1705128.

42. Hou, L., Wang, N., Man, X., Cui, Z., Wu, J., Liu, J., Li, S., Gao, Y., Li, D., Jiang, L., and Zhao, Y. (2019). Interpenetrating Janus membrane for high rectification ratio liquid unidirectional penetration. ACS Nano *13*, 4124–4132.

43. Shi, L., Liu, X., Wang, W., Jiang, L., and Wang, S. (2019). A self-pumping dressing for draining excessive biofluid around wounds. Adv. Mater. *31*, e1804187.

44. Choi, W., Tuteja, A., Chhatre, S., Mabry, J.M., Cohen, R.E., and McKinley, G.H.J.A.M. (2009). Fabrics with tunable oleophobicity. Adv. Mater. *21*, 2190–2195.

45. Cheng, Z., Wang, B., Lai, H., Liu, P., Zhang, D., Tian, D., Liu, H., Yu, X., Sun, B., and Sun, K. (2017). Janus copper mesh film with unidirectional water transportation ability toward high efficiency oil/water separation. Chem. Asian J. *12*, 2085–2092.

46. Liu, L., Bakhshi, H., Jiang, S., Schmalz, H., and Agarwal, S. (2018). Composite polymeric membranes with directionally embedded fibers for controlled dual actuation. Macromol. Rapid Commun. *39*, e1800082.

47. Duan, G., and Greiner, A. (2019). Air-blowing-assisted coaxial electrospinning toward high productivity of Core/sheath and hollow fibers. Macromol. Mater. Eng. *304*, 1800669.

48. Shou, D., and Fan, J. (2018). An all hydrophilic fluid diode for unidirectional flow in porous systems. Adv. Funct. Mater. *28*, 1800269.

49. Wu, J., Wang, N., Wang, L., Dong, H., Zhao, Y., and Jiang, L. (2012). Unidirectional water-penetration composite fibrous film via electrospinning. Soft Matter *8*, 5996–5999.

50. Wang, Y., Liang, X., Zhu, H., Xin, J.H., Zhang, Q., and Zhu, S. (2020). Reversible water transportation diode: Temperature-adaptive smart Janus textile for moisture/thermal management. Adv. Funct. Mater. *30*, 1907851.

51. Kong, Y.Y., and Xin, J.H. (2018). Janus fabric with self-propelled directional wetting patterns induced by light and temperature. Adv. Eng. Mater. *20*, 1700905.

52. Tian, Y., Zhu, P., Tang, X., Zhou, C., Wang, J., Kong, T., Xu, M., and Wang, L. (2017). Large-scale water collection of bioinspired cavity-microfibers. Nat. Commun. *8*, 1080.

53. Lorenceau, É., and Quéré, D. (2004). Drops on a conical wire. J. Fluid Mech. *510*, 29–45.

54. Shang, L., Cheng, Y., and Zhao, Y. (2017). Emerging droplet microfluidics. Chem. Rev. *117*, 7964–8040.

55. Mason, G., and Morrow, N.R. (1984). Meniscus curvatures in capillaries of uniform cross-section. J. Chem. Soc. Faraday Trans. 1. *80*, 2375–2393.

56. Herminghaus, S., Brinkmann, M., and Seemann, R. (2008). Wetting and dewetting of complex surface geometries. Annu. Rev. Mater. Res. *38*, 101–121.

57. Shou, D., Ye, L., Fan, J., and Fu, K. (2014). Optimal design of porous structures for the fastest liquid absorption. Langmuir *30*, 149–155.

58. Shou, D., Ye, L., Fan, J., Fu, K., Mei, M., Wang, H., and Chen, Q. (2014). Geometry-induced asymmetric capillary flow. Langmuir *30*, 5448–5454.

59. Li, J., Song, Y., Zheng, H., Feng, S., Xu, W., and Wang, Z. (2019). Designing biomimetic liquid diodes. Soft Matter *15*, 1902–1915.

60. Cao, M., Li, K., Dong, Z., Yu, C., Yang, S., Song, C., Liu, K., and Jiang, L. (2015). Superhydrophobic "pump": Continuous and spontaneous antigravity water delivery. Adv. Funct. Mater. *25*, 4114–4119.

61. Zhou, H., Wang, H., Niu, H., and Lin, T. (2013). Superphobicity/philicity Janus fabrics with switchable, spontaneous, directional transport ability to water and oil fluids. Sci. Rep. *3*, 2964.

62. Wang, H., Zhou, H., Niu, H., Zhang, J., Du, Y., and Lin, T. (2015). Dual-layer superamphiphobic/superhydrophobic-oleophilic nanofibrous membranes with unidirectional oil-transport ability and strengthened oil–water separation performance. Adv. Mater. Interfaces *2*, 1400506.

63. Wang, H., Ding, J., Dai, L., Wang, X., and Lin, T. (2010). Directional water-transfer through fabrics induced by asymmetric wettability. J. Mater. Chem. *20*, 7938–7940.

64. Zhang, Q., Li, Y., Yan, Y., Zhang, X., Tian, D., and Jiang, L. (2020). Highly flexible monolayered porous membrane with superhydrophilicity-hydrophilicity for unidirectional liquid penetration. ACS Nano *14*, 7287–7296.

65. Tuteja, A., Choi, W., Ma, M., Mabry, J.M., Mazzella, S.A., Rutledge, G.C., McKinley, G.H., and Cohen, R.E. (2007). Designing superoleophobic surfaces. Science *318*, 1618–1622.

66. Luo, C., Heng, X., and Xiang, M. (2014). Behavior of a liquid drop between two nonparallel plates. Langmuir *30*, 8373–8380.

67. Jiang, Y., Hou, J., Xu, J., and Shan, B. (2017). Switchable oil/water separation with efficient and robust Janus nanofiber membranes. Carbon *115*, 477–485.

68. Zhang, Z., Zhang, Y., Fan, H., Wang, Y., Zhou, C., Ren, F., Wu, S., Li, G., Hu, Y., Li, J., et al. (2017). A Janus oil barrel with tapered microhole arrays for spontaneous high-flux spilled oil absorption and storage. Nanoscale *9*, 15796–15803.

69. An, Y.-P., Yang, J., Yang, H.-C., Wu, M.-B., and Xu, Z.-K. (2018). Janus membranes with charged carbon nanotube coatings for deemulsification and separation of oil-in-water emulsions. ACS Appl. Mater. Interfaces *10*, 9832–9840.

70. Yang, H.-C., Zhong, W., Hou, J., Chen, V., and Xu, Z.-K. (2017). Janus hollow fiber membrane with a mussel-inspired coating on the lumen surface for direct contact membrane distillation. J. Membr. Sci. *523*, 1–7.

71. Huang, Y.-X., Wang, Z., Jin, J., and Lin, S. (2017). Novel Janus membrane for membrane distillation with simultaneous fouling and wetting resistance. Environ. Sci. Technol. *51*, 13304–13310.

72. Feng, S., Xing, Y., Deng, S., Shang, W., Li, D., Zhang, M., Hou, Y., and Zheng, Y. (2018). An integrative mesh with dual wettable on–off switch of water/oil. Adv. Mater. Interfaces *5*, 1701193.

73. Ren, F., Li, G., Zhang, Z., Zhang, X., Fan, H., Zhou, C., Wang, Y., Zhang, Y., Wang, C., and Mu, K. (2017). A single-layer Janus membrane with dual gradient conical micropore arrays for self-driving fog collection. J. Mater. Chem. A. *5*, 18403–18408.

74. Gupta, P., and Kandasubramanian, B. (2017). Directional fluid gating by janus membranes with heterogeneous wetting properties for selective oil–water separation. ACS Appl. Mater. Interfaces *9*, 19102–19113.

75. Wang, Z., Wang, Y., and Liu, G. (2016). Rapid and efficient separation of oil from oil-in-water emulsions using a Janus cotton fabric. Angew. Chem. Int. Ed. Engl. *55*, 1291–1294.

76. Huang, G., Liang, Y., Wang, J., Zeng, X., Li, Z., and Zhang, X. (2019). Effect of asymmetric wettability on directional transport of water through Janus fabrics prepared by an electrospinning technique. Mater. Lett. *246*, 76–79.

77. Hu, R., Wang, N., Hou, L., Cui, Z., Liu, J., Li, D., Li, Q., Zhang, H., and Zhao, Y. (2019). A bioinspired hybrid membrane with wettability and topology anisotropy for highly efficient fog collection. J. Mater. Chem. A. *7*, 124–132.

78. Lv, C., Chen, C., Chuang, Y.-C., Tseng, F.-G., Yin, Y., Grey, F., and Zheng, Q. (2014). Substrate curvature gradient drives rapid droplet motion. Phys. Rev. Lett. *113*, 026101.

79. Li, S., Liu, J., and Hou, J. (2016). Curvature-driven bubbles or droplets on the spiral surface. Sci. Rep. *6*, 37888.

80. Ainla, A., Hamedi, M.M., Güder, F., and Whitesides, G.M. (2017). Electrical textile valves for paper microfluidics. Adv. Mater. *29*, 1702894.

81. Koşak Söz, Ç., Trosien, S., and Biesalski, M. (2018). Superhydrophobic hybrid paper sheets with Janus-type wettability. ACS Appl. Mater. Interfaces *10*, 37478–37488.

82. Lim, H.S., Park, S.H., Koo, S.H., Kwark, Y.-J., Thomas, E.L., Jeong, Y., and Cho, J.H. (2010). Superamphiphilic Janus fabric. Langmuir *26*, 19159–19162.

83. Tian, X., Jin, H., Sainio, J., Ras, R.H., and Ikkala, O. (2014). Droplet and fluid gating by biomimetic janus membranes. Adv. Funct. Mater. *24*, 6023–6028.

84. Prabu, G., Chattopadhyay, S.K., Patil, P.G., Arputharaj, A., Mandhyan, P., Prasad, G.K., Vivekanandan, M., Hadge, G.B., and Nadanathangam, V. (2017). Moisture management finish on cotton fabric by electrospraying. Text. Res. J. *87*, 2154–2165.

85. Gore, P.M., Dhanshetty, M., and Balasubramanian, K. (2016). Bionic creation of nano-engineered Janus fabric for selective oil/organic solvent absorption. RSC Adv. *6*, 111250–111260.

86. Zhu, T., Wu, J., Zhao, N., Cai, C., Qian, Z., Si, F., Luo, H., Guo, J., Lai, X., Shao, L., and Xu, J. (2018). Superhydrophobic/superhydrophilic janus fabrics reducing blood loss. Adv. Healthc. Mater. *7*, e1701086.

87. Sasaki, K., Tenjimbayashi, M., Manabe, K., and Shiratori, S. (2016). Asymmetric superhydrophobic/superhydrophilic cotton fabrics designed by spraying polymer and nanoparticles. ACS Appl. Mater. Interfaces *8*, 651–659.

88. An, Y.H., Yu, S.J., Kim, I.S., Kim, S.H., Moon, J.M., Kim, S.L., Choi, Y.H., Choi, J.S., Im, S.G., Lee, K.E., and Hwang, N.S. (2017). Hydrogel functionalized Janus membrane for skin regeneration. Adv. Healthc. Mater. *6*, 1600795.

89. Postulka, N., Striegel, A., Kraußе, M., Mager, D., Spiehl, D., Meckel, T., Worgull, M., and Biesalski, M. (2019). Combining wax printing with hot embossing for the design of geometrically well-defined microfluidic papers. ACS Appl. Mater. Interfaces *11*, 4578–4587.

90. Tian, P., Gao, X., Wen, G., Zhong, L., Wang, Z., and Guo, Z. (2018). Novel fabrication of polymer/carbon nanotube composite coated

Janus paper for humidity stress sensor. J. Colloid Interface Sci. *532*, 517–526.

91. Liang, Y., Huang, G., Zeng, X., Li, Z., Zou, J., and Li, X. (2020). Effects of hydrophilic layer on directional transport of water through robust tri-layered Janus fabrics prepared by electrospinning. Mater. Lett. *268*, 127583.

92. Söz, C.K.a., Trosien, S., and Biesalski, M. (2020). Janus interface materials: a critical review and comparative study. ACS Materials Letters *2*, 336–357.

93. Zhou, S., Liu, F., Wang, J., Lin, H., Han, Q., Zhao, S., and Tang, C.Y. (2019). Janus membrane with unparalleled forward osmosis performance. Environ. Sci. Technol. Lett. *6*, 79–85.

94. Miao, L., Liu, G., and Wang, J. (2019). Ag-nanoparticle-bearing poly (vinylidene fluoride) nanofiber mats as janus filters for catalysis and separation. ACS Appl. Mater. Interfaces *11*, 7397–7404.

95. Zheng, S., Li, C., Fu, Q., Li, M., Hu, W., Wang, Q., Du, M., Liu, X., and Chen, Z. (2015). Fabrication of self-cleaning superhydrophobic surface on aluminum alloys with excellent corrosion resistance. Surf. Coat. Tech. *276*, 341–348.

96. Cao, M., Xiao, J., Yu, C., Li, K., and Jiang, L. (2015). Hydrophobic/hydrophilic cooperative Janus system for enhancement of fog collection. Small *11*, 4379–4384.

97. Riveiro, A., Pou, P., del Val, J., Comesaña, R., Arias-González, F., Lusquiños, F., Boutinguiza, M., Quintero, F., Badaoui, A., and Pou, J. (2020). Laser texturing to control the wettability of materials. Procedia CIRP *94*, 879–884.

98. Sparavigna, A. (2008). Plasma treatment advantages for textiles. arXiv, 0801.3727. https://arxiv.org/abs/0801.3727.

99. Pionteck, J., Pionteck, J., and Wypych, G. (2007). Handbook of antistatics (ChemTec Publishing).

100. Riveiro, A., Abalde, T., Pou, P., Soto, R., del Val, J., Comesaña, R., Badaoui, A., Boutinguiza, M., and Pou, J. (2020). Influence of laser texturing on the wettability of PTFE. Appl. Surf. Sci. *515*, 145984.

101. Wagner, N., and Theato, P. (2014). Light-induced wettability changes on polymer surfaces. Polymer *55*, 3436–3453.

102. Gotoh, K., Yasukawa, A., and Kobayashi, Y. (2011). Wettability characteristics of poly (ethylene terephthalate) films treated by atmospheric pressure plasma and ultraviolet excimer light. Polym. J. *43*, 545–551.

103. Agarwal, S., Wendorff, J.H., and Greiner, A. (2008). Use of electrospinning technique for biomedical applications. Polymer *49*, 5603–5621.

104. Shi, X., Zhou, W., Ma, D., Ma, Q., Bridges, D., Ma, Y., and Hu, A. (2015). Electrospinning of nanofibers and their applications for energy devices. J. Nanomater. *2015*, 140716.

105. Ju, J., Shi, Z., Deng, N., Liang, Y., Kang, W., and Cheng, B. (2017). Designing waterproof breathable material with moisture unidirectional transport characteristics based on a TPU/TBAC tree-like and TPU nanofiber double-layer membrane fabricated by electrospinning. RSC Adv. *7*, 32155–32163.

106. Gorji, M., Karimi, M., and Nasheroahkam, S. (2018). Electrospun PU/P (AMPS-GO) nanofibrous membrane with dual-mode hydrophobic–hydrophilic properties for protective clothing applications. J. Ind. Text. *47*, 1166–1184.

107. Li, C., Dai, H., Gao, C., Wang, T., Dong, Z., and Jiang, L. (2019). Bioinspired inner microstructured tube controlled capillary rise. Proc. Natl. Acad. Sci. USA *116*, 12704–12709.

108. Park, K.-C., Kim, P., Grinthal, A., He, N., Fox, D., Weaver, J.C., and Aizenberg, J. (2016). Condensation on slippery asymmetric bumps. Nature *531*, 78–82.

109. Yetisen, A.K., Qu, H., Manbachi, A., Butt, H., Dokmeci, M.R., Hinestroza, J.P., Skorobogatiy, M., Khademhosseini, A., and Yun, S.H. (2016). Nanotechnology in textiles. ACS Nano *10*, 3042–3068.

110. Gore, R.W. (1976). Process for Producing Porous Products (Google Patents).

111. Babar, A.A., Wang, X., Iqbal, N., Yu, J., and Ding, B. (2017). Tailoring differential moisture transfer performance of nonwoven/polyacrylonitrile-SiO2 nanofiber composite membranes. Adv. Mater. Interfaces *4*, 1700062.

112. Bagherzadeh, R., Gorji, M., Latifi, M., Payvandy, P., and Kong, L.X. (2012). Evolution of moisture management behavior of high-wicking 3D warp knitted spacer fabrics. Fibers Polym. *13*, 529–534.

113. Zimmermann, J., Reifler, F.A., Fortunato, G., Gerhardt, L.C., and Seeger, S. (2008). A simple, one-step approach to durable and robust superhydrophobic textiles. Adv. Funct. Mater. *18*, 3662–3669.

114. Zaman, M., Liu, H., Xiao, H., Chibante, F., and Ni, Y. (2013). Hydrophilic modification of polyester fabric by applying nanocrystalline cellulose containing surface finish. Carbohydr. Polym. *91*, 560–567.

115. Mukhopadhyay, A., and Midha, V.K. (2008). A review on designing the waterproof breathable fabrics part II: Construction and suitability of breathable fabrics for different uses. J. Ind. Text. *38*, 17–41.

116. Comanns, P., Effertz, C., Hischen, F., Staudt, K., Böhme, W., and Baumgartner, W. (2011). Moisture harvesting and water transport through specialized micro-structures on the integument of lizards. Beilstein J. Nanotechnol. *2*, 204–214.

117. Bai, H., Wang, L., Ju, J., Sun, R., Zheng, Y., and Jiang, L. (2014). Efficient water collection on integrative bioinspired surfaces with star-shaped wettability patterns. Adv. Mater. *26*, 5025–5030.

118. Brown, P.S., and Bhushan, B. (2016). Bioinspired materials for water supply and management: water collection, water purification and separation of water from oil. Philos. Trans.- Royal Soc., Math. Phys. Eng. Sci. *374*, 20160135.

119. Liu, Y., Qu, R., Zhang, W., Li, X., Wei, Y., and Feng, L. (2019). Lotus-and mussel-inspired PDA–PET/PTFE Janus membrane: toward integrated separation of light and heavy oils from water. ACS Appl. Mater. Interfaces *11*, 20545–20556.

120. Nau, M., Herzog, N., Schmidt, J., Meckel, T., Andrieu-Brunsen, A., and Biesalski, M. (2019). Janus-type hybrid paper membranes. Adv. Mater. Interfaces *6*, 1900892.

121. Yun, J., Khan, F.A., and Baik, S. (2017). Janus graphene oxide sponges for high-purity fast separation of both water-in-oil and oil-in-water emulsions. ACS Appl. Mater. Interfaces *9*, 16694–16703.

122. Liang, Y., Kim, S., Kallem, P., and Choi, H. (2019). Capillary effect in Janus electrospun nanofiber membrane for oil/water emulsion separation. Chemosphere *221*, 479–485.

123. Wang, Z., Lehtinen, M., and Liu, G. (2017). Universal Janus filters for the rapid separation of oil from emulsions stabilized by ionic or nonionic surfactants. Angew. Chem. Int. Ed. Engl. *56*, 12892–12897.

124. Zhang, Y., Cao, M., Peng, Y., Jin, X., Tian, D., Liu, K., and Jiang, L. (2018). Directional transport: Bioinspired continuous and spontaneous antigravity oil collection and transportation. Adv. Funct. Mater. *28*, 1870032.

125. Yue, X., Zhang, T., Yang, D., Qiu, F., and Li, Z. (2018). Janus ZnO-cellulose/MnO 2 hybrid membranes with asymmetric wettability for highly-efficient emulsion separations. Cellulose *25*, 5951–5965.

126. Zhu, Y., Tian, G., Liu, Y., Li, H., Zhang, P., Zhan, L., Gao, R., and Huang, C. (2021). Low-cost, unsinkable, and highly efficient solar evaporators based on coating MWCNTs on nonwovens with unidirectional water-transfer. Adv. Sci. *8*, 2101727.

127. Shou, D., Ye, L., Tang, Y., Fan, J., and Ding, F. (2013). Transverse permeability determination of dual-scale fibrous materials. Int. J. Heat Mass Transf. *58*, 532–539.

128. Shou, D., Fan, J., and Ding, F. (2011). Hydraulic permeability of fibrous porous media. Int. J. Heat Mass Transf. *54*, 4009–4018.

129. Kwon, G., Panchanathan, D., Mahmoudi, S.R., Gondal, M.A., McKinley, G.H., and Varanasi, K.K. (2017). Visible light guided manipulation of liquid wettability on photoresponsive surfaces. Nat. Commun. *8*, 14968.

130. Lv, J.A., Liu, Y., Wei, J., Chen, E., Qin, L., and Yu, Y. (2016). Photocontrol of fluid slugs in liquid crystal polymer microactuators. Nature *537*, 179–184.

131. Wegst, U.G., Bai, H., Saiz, E., Tomsia, A.P., and Ritchie, R.O. (2015). Bioinspired structural materials. Nat. Mater. *14*, 23–36.

132. Truby, R.L., and Lewis, J.A. (2016). Printing soft matter in three dimensions. Nature *540*, 371–378.

133. Zhang, Y., Zhang, F., Yan, Z., Ma, Q., Li, X., Huang, Y., and Rogers, J.A. (2017). Printing, folding and assembly methods for forming 3D

mesostructures in advanced materials. Nat. Rev. Mater. *2*, 1–17.

134. Zhou, H., Wang, H., Niu, H., Gestos, A., Wang, X., and Lin, T. (2012). Fluoroalkyl silane modified silicone rubber/nanoparticle composite: a super durable, robust superhydrophobic fabric coating. Adv. Mater. *24*, 2409–2412.

135. Deng, B., Cai, R., Yu, Y., Jiang, H., Wang, C., Li, J., Li, L., Yu, M., Li, J., Xie, L., et al. (2010). Laundering durability of superhydrophobic cotton fabric. Adv. Mater. *22*, 5473–5477.

136. Baidya, A., Ganayee, M.A., Jakka Ravindran, S., Tam, K.C., Das, S.K., Ras, R.H.A., and Pradeep, T. (2017). Organic solvent-free fabrication of durable and multifunctional superhydrophobic paper from waterborne fluorinated cellulose nanofiber building blocks. ACS Nano *11*, 11091–11099.

137. Vierke, L., Staude, C., Biegel-Engler, A., Drost, W., and Schulte, C. (2012). Perfluorooctanoic acid (PFOA)—main concerns and regulatory developments in Europe from an environmental point of view. Environ. Sci. Eur. *24*, 1–11.

138. Schultz, M.M., Barofsky, D.F., and Field, J.A. (2003). Fluorinated alkyl surfactants. Environ. Eng. Sci. *20*, 487–501.